PROPOSAL FOR AN INFN EXPERIMENT
2013 - 2015

ELIMED:
MEDical applications at ELI-Beamlines

August 17, 2012

CONTENTS

1 Project overview

Proposal name	ELIMED
Involved INFN Sections	LNS, LNL, INFN-CT, INFN-BO
National responsibles	G A Pablo Cirrone and L Torrisi (INFN-LNS)
External participants:	Drug Sciences Department, University of Catania, Catania (I); School of Mathematics and Physics, Queen's University of Belfast, Belfast (UK); ELI Experimental Program Department, Institute of Physics of the ASCR, Prague, (CZ); Russian Academy of Science, Moscow (RU); Vinca Institute of Nuclear Sciences, University of Belgrade, Belgrade (Serbia)
Temporal schedule	3 years (2013 - 2015)

1.1 Short description

The project aim is the development of innovative instrumentation, technologies and new methodologies for dosimetry and radiobiology in order to realize an hadrontherapy facility based on laser-driven beams. The project will closely follow the activities of the ELIMED project that will realize a hadrontherapy transport beam line using laser-driven beams accelerated at the ELI-Beamlines laser facility in Prague (CZ). One of the project main goals will be the realization of a first prototype of energy selector for laser-driven proton beams and of the necessary diagnostic systems in order to perform the first dosimetric and radiobiological measures at three different laser facilities: the TARANIS laser facility in Belfast (UK), the GIST, Gwangju in Korea and the FLAME laser in Frascati (I).
Part of the developed diagnostic will be also tested at the PALS facility in Prague (CZ).

2 INTRODUCTION

At INFN-LNS since many years three exceptional, well-established research areas coexist: ion acceleration and beam transport, plasma ion acceleration and related diagnostic, hadrontherapy and medical physics applications. This favorable presence allowed us to launch in the past months the European ELIMED initiative. ELIMED, acronym of MEDical applications at ELI-Beamlines, is an international venture started by a joined collaboration between INFN-LNS and ELI Experimental Program Department (Prague) researchers. The main aim of the project is the realisation, within the year 2018, of the first facility entirely dedicated to the physics and radiobiological studies of high-energy (60 - 250 MeV) proton beams accelerated by the high-power laser interaction with matter. As reported in many theoretical studies as well as in a vast set of experiments with lower power laser systems, the produced beams will show very peculiar energy spectrum, fluence and temporal distributions. In particular lasers with a very short duration generate extremely intense pulsed beams ($10^9 - 10^{12}$ protons per pulse with 1.0 - 0.1 nsec pulse duration). ELIMED will be a specific laser facility designed and realised with the aim to demonstrate the clinical applicability of these laser-driven proton beams (up to 20 - 30 MeV of kinetic energy in the first phase). Particular care will be devoted to the design, development and test all of the diagnostic devices necessary to monitor the different phases of the particles production (from the laser-target interaction point to the final clinical beam). A specific effort will be dedicated to the dosimetric and radiobiology studies. They will lead to the development of innovative detectors able to perform absolute and relative dose measurements to be used for a quantitative evaluation of the biological effects of the laser-driven beams compared to conventionally accelerated particles. ELIMED will therefore represent the first step towards a feasible reduction in dimensions and costs of future hadrontherapy facilities. From a pure scientific point of view, it will also represent a key opportunity for different and multidisciplinary research activities to converge and for the development of innovative detection techniques and to study and characterise this new kind of beams.

The ELIMED Collaboration is now growing and different research institutes are joining it or expressing the will of an active participation. The list of the actual European ELIMED partners can be found in the Section 1 of this proposal.

The scientific collaboration between INFN-LNS and ELI-Beamlines has been made official through a Memorandum of Understanding (MoU) signed in April 2012. The MoU establishes the scientific program, the time schedule and the specific responsibilities of the two research institutes in connection with the ELIMED Collaboration. A copy of the signed MoU is attached to this proposal. Starting from these considerations, taking in account the extreme novelty and originality of the ELIMED activity and also the interest shown by the INFN in this field (funds of laser-plasma related projects, development and realisation of the FLAME facility at LNF, disposal into the MoU sign, etc.) we decide to submit to the INFN Fifth Commission this new proposal that we are calling ELIMED.

3 The ELIMED facility at ELI-Beamlines

The ELIMED European Collaboration is planning the realisation, at ELI-Beamline facility in Prague, of a specific transport beam line to study the potential medical applications of the laser-accelerated ions. ELI-beamlines is one of the four pillars of the pan-European ELI infrastructure (funded in the framework of the European ESFRI process) which is planning the realisation of four different high power (up to 200 PW) laser facilities that will be located in four different European countries. The Prague facility, in particular, named ELI-Beamlines, will be entirely dedicated to the study of the potential applications of the secondary sources (like more energetic ion beams) generated by these lasers class. Of course, one of the potential application of ion sources is the external cancer radiation treatment or hadrontherapy. ELIMED was born by a common initiative proposed by researches of the INFN-LNS in Catania and FZU (Academy of Sciences of Czech Republic) in Prague. The starting idea was the wish to demonstrate the clinical applicability of the laser-driven protons. The proposed initiative has been favorably approved by the scientific committee of ELI-Beamlines and now ELIMED has a dedicated room (Experimental Hall number 6) specifically assigned for the realisation of the medical beam-line. The room will have a surface of about 50 m^2. It will contain the interaction chamber (where the laser impacts on the target), the energy selection system and, finally, the in-air hadrontherapy transport beam line with the connected dosimetric devices. Figure 3.1 shows a graphical layout of the ELI-Beamline structure. Experimental halls are located at the lower floor.

The temporal development of the European ELIMED project will be constituted of four different stages, each related to a well defined phase of the ELI-Beamlines facility development: These phases are:

1. ***The preliminary phase (2013 - 2016)***: during this phase the ELI-Beamline facility will be realised and no laser-driven beam will be available. In this period all the aspects will be analyzed and the first prototype of beam transport and selection systems, detectors and dosimetry will be designed and realized. Preliminary experimental runs with the realized devices will be performed in facilities where laser-driven ions beams are already available even if at lower energies.

Figure 3.1: Graphical overview of the ELI-Beamlines facility. The Exp hall 6 is the one dedicated to the ELIMED project

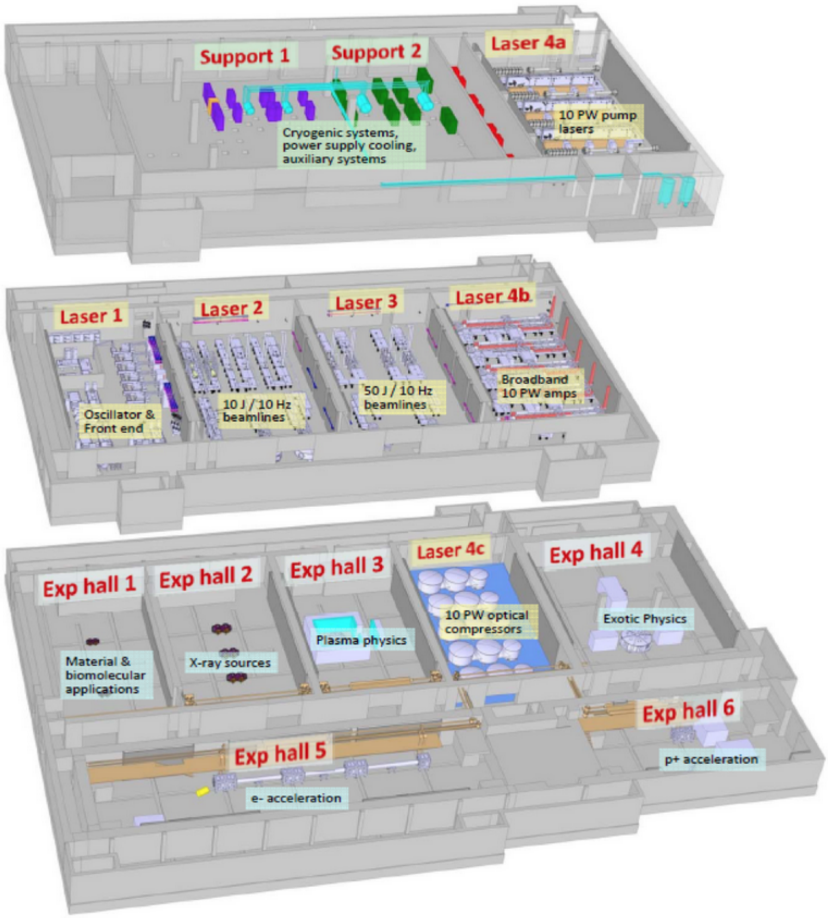

2. ***Phase 1 (2016-2017)***: first laser shots will be available and protons in the 20-30 MeV energy range are expected. The energy selection system would be installed and the first dosimetric studies and cell irradiation could be performed.

3. ***Phase 2 (2017-2019)***: 60 - 200 MeV proton beams are expected after the target. The final configuration of the in-air hadrontherapy transport beam line would be assembled and tested. Final dosimetric characterisation and radiobiological tests would be performed.

4. ***Phase 3 (starting since 2020)***: proton beams with a maximum energy of 1 GeV are expected.

In Table 3.1 the laser system and produced ion beams characteristics we expect at the various ELIMED phases are summarized. In the same Table the estimation of the expected beam characteristics after the energy selection system and dose evaluation at the irradiation point are presented.

Table 3.1: Laser and and laser-driven beams expected at the ELIMED facility in the various phases.

	Phase 1	**Phase 2**	**Phase 3**
Focused intensity $[W/cm^2]$	$10^{19} - 5 \cdot 10^{21}$	$5 \cdot 10^{19} - 10^{23}$	$5 \cdot 10^{19} - 10^{23}$
Energy range [MeV]	20 - 30	60 - 200	100 - 1000
No particle per shot	$10^{9} - 10^{10}$	$10^{10} - 10^{11}$	$10^{11} - 10^{12}$
Bunch duration [nsec]	1	0.1 - 1	< 0.1
Protons per pulse after the beam transport	$5 \cdot 10^{8} - 5 \cdot 10^{10}$	$5 \cdot 10^{9} - 5 \cdot 10^{10}$	$\sim 10^{11}$
Energy spread	±5%	±5%	not still defined
Proton dose per shot to the cells	0.1 - 1 Gy	0.06 - 0.6 Gy	~ 7 Gy per shot

4 RELEVANCE OF THE PROJECT WITH RESPECT TO THE INFN MISSION AND THE STATE OF THE ART OF THE PROPOSED RESEARCH

The scientific interest of INFN for hadrontherapy and all the related topics is evident. INFN, that is leader in research and development of accelerator machines, has funded in the last twenty years various initiatives related to hadronterapy. INFN supported and realized the first Italian proton therapy center at the LNS Laboratory in Catania that is still active and have

treated more than 300 patients up to now. Starting from 2004 the INFN signed an agreement with the CNAO foundation to actively participate in the realisation of the first Hospital-based Italian hadrontherapy center. The relevance of hadrontherapy and related topics for INFN is also widely declared inside the INFN triennial scientific plan (years 2012 - 2014) [1]. In the same document the study, design and realisation of a therapy beam line for the laser-driven beams is expressly reported as one of the LNS milestones for the period 2012 - 2014. In our opinion is hence evident that the scientific activity we are proposing, perfectly fits with the scientific INFN mission.
Nowadays the international panorama saws the German OncoRay (http://www.oncoray.de/) and Light (http://nnp.physik.uni-frankfurt.de/Light/) projects and the PMRC (Photo Medical Research Center) activity in Japan (even if for the last one, financial support from the Japan government have been momentarily stopped). These three initiatives are strongly working onto the topics related with the future use of the laser-driven protons for therapy purposes and they express, together with the ELIMED project, the status of the art in this field.

5 Project aim and implementation

The activity of the INFN ELIMED project will be entirely focused on the development of innovative instrumentation, technologies and dosimetric methodologies pointed to the development of a beam line for dosimetric and radiobiological studies based on laser-driven beams with energy of interest in hadrontherapy. The project will closely follow the activities of the ELIMED project that will accomplish, within 2017, the first beam line for therapy studies using laser-driven beams accelerated up to 30 MeV at the ELI-Beamlines laser facility in Prague (CZ). One of the main goal of the project will be the realization of a first prototype of energy selector for laser-driven proton beams and the necessary diagnostic systems in order to perform the first dosimetric and radiobiological measurements at three different laser facilities: the TARANIS laser facility in Belfast (UK), the GIST in Korea and FLAME laser in Frascati (IT). Evidently, one of the intrinsic characteristics of the ELIMED project is its multidisciplinary approach. The realisation of a transport beam line for hadrontherapy studies based on laser-driven beams, in fact, requires many different competences. People with knowledge of targets design and realisation, of plasma characterisation, of the emitted radiation diagnostic from the target, of the selection and transport of the produced charged beam as well as of the dosimetric, radiobiological and beam formation for hadrontherapy, will be involved simultaneously. In the same way, people skilled in the simulation of high power lasers interaction with the matter using realistic Particle In Cell (PIC) codes, are necessary. In the preliminary phases in fact, the theoretical knowledge of the produced radiation from the targets (in terms of energy, fluence and momentum distributions) will be of topical importance. It will firstly give us the possibility to evaluate the performances of systems and detectors we are planning to experimentally test with laser-driven beams. Secondly, it will give us the possibility to simulate the whole beam line from the target, through the selection system and up to the dosimetry and biologic irradiation point.

We are organizing our proposal in such a way that all these different aspects can be considered and sufficiently and coherently investigated. In order to achieve this objective, researchers with competences in the different involved areas have been joined together to form a complete team having the same scientific goal. The ELIMED scientific proposal have been divided in three Working Packages (WP), each of them dedicated to a specific research aspect of interest for the project. Each WP has its main responsible and it is in turn divided in smaller sub-WPs. The WP-1 is dedicated to all the aspects related to the target design and realisation, to the plasma and to the diagnostic of the produced radiation and to the development of PIC simulations. The WP-2 is fully related to the design and realisation of the energy selection and transport of the produced proton beams. Finally the WP-3 will investigate all the problematics related to the development and test of new dosimetric systems, to design of the in-air transport proton beam line, to the absolute and relative dosimetry issues and to the radiobiological tests.
Figure 5.1 shows the ELIMED transport beam line as it is designed at the moment. It is divided in three parts and activities in each of them will be covered by a different and specific WP.

In order to rigorously define our research activity timeline, we assigned to each WP a set of well defined and detailed milestones and deliverables. These will be discussed with more details in the paragraph Milestones, deriverables and temporal plan. We estimated that the project activity can be completed in three years, with our actual Full Time Equivalent manpower that is about 18.0.

6 Participation of external agencies contributing to the project funds

The project will be financially supported by the FZU AS CR in Prague that will contribute with 1-2 PhD, 1 three-years post-doc to work on the energy selection system and on the preparation of the Belfast experimental run and, finally, into travel expenses for the part of the people that will perform the planned experimental runs at PALS (Prague), TARANIS (Belfast), GIST (Korea) and FLAME (Italy) laser facilities. At the time in which we are writing, a five-months contract for a technical designer and one half of the travel expenses for a preliminary experimental measure at PALS have been already provided by FZU. The post-doc public announcement has

Figure 5.1: Schematic layout of the ELIMED final beam line as it will be implemented at the ELI-Beamlines in Prague. The scientific activity we are proposing is divided in three parts each corresponding to a specific section of the beam line and to a well defined Working Package.

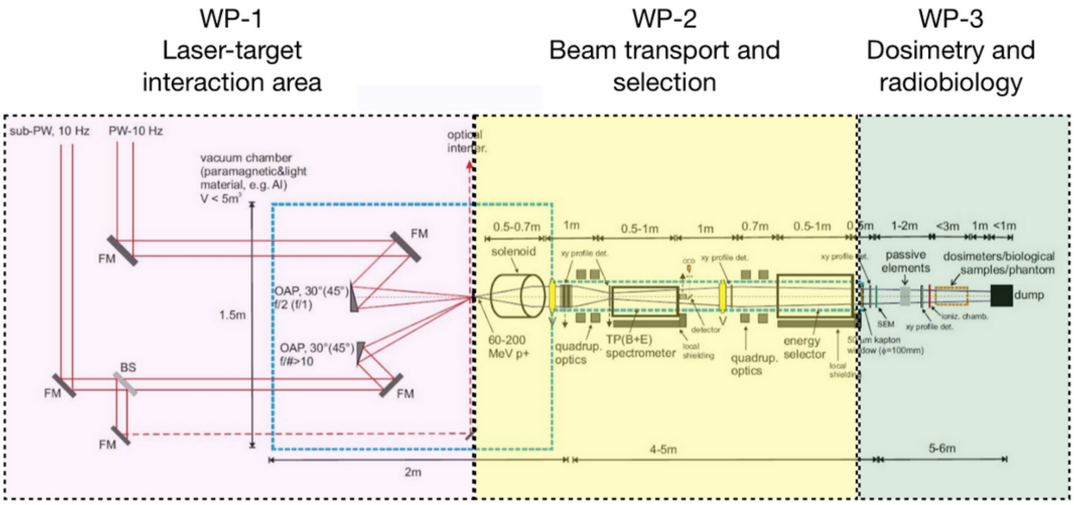

been provided and the deadline fixed for July the 2nd, 2012. We expect to start the contract on September 2012. Support will be also provided for the 2013 experimental run at PALS (already assigned) where travel expenses will be covered for four participants and for the full experiment duration (three weeks).

One will be the Queen's University in Belfast that already gave the full disposal in providing us a set of experimental shifts with the TARANIS laser system there installed. At the same time they will provide us also the full technical support. The disposal of the Queen's University is documented with a letter attached to this proposal. In the same way we will have the access to the PALS femtosecond laser system for the final test of the improved Thomson Spectrometer. Additional contributes will be provided by the Drugs Department of Catania University that will support the radiobiological measurements making at their laboratories available for cells culture and analysis as well as their scientific expertise. Based on more than a decade long collaboration and experience in irradiations with protons and carbon ions of biological samples at LNS, group of researchers (nuclear physicists and molecular biologists) from the Vinca Institute of Nuclear Sciences, University of Belgrade, will give their contribute in the field of radiobiology.

7 PROJECT WORKING PLAN

ELIMED scientific activity is organised in Working Packages (WPs). Each WP corresponds to a well defined research activity in turn connected with those will be performed at ELI-Beamlines.

WP-1: Target, PIC simulations, plasma and laser-driven beam diagnostic

WP Responsible: Dr. A. Anzalone

WP - 1.1: Targets development and optimisation for proton productions. Quantitative evaluation of accelerated particles using Particle In Cell (PIC) simulations.

WP - 1.2: Charged beams diagnostic: upgrade of INFN Thomson spectrometer for the diagnostic of charged beams up to 100 AMeV; CR39, SIC, Synthetic Mono-crystal Diamond Detector, Ion Collector (IC) and Ion Collector Ring (ICR); electron detectors.
Feasibility studies of a new Thomson spectrometer for beam energies up to 100 MeV.

WP - 1.3: Optical and UV imaging and spectroscopy.

WP - 1.4: X-spectroscopy and imaging.

WP-2: Energy selection system and beam transport

WP Responsible: Dr. M. Maggiore

WP - 2.1: Feasibility studies of innovative energy selection and beam transport systems to transform the laser generated mixed beam in a clinical one.

WP - 2.2: Monte Carlo simulations of the energy selection system.

WP - 2.3: First prototype of an energy selection system up to 50 MeV.

WP-3: Hadrontherapy transport, dosimetry and radiobiology

WP Responsible: Dr. F. Romano

WP - 3.1: Evaluation of the coming-out beams dose distributions and of the secondary radiation generated inside the selection system; design and Monte Carlo simulations of transport beam line from the selection system and related radioprotection evaluations.

WP - 3.2: Development of innovative systems for in-air diagnostic of accelerated particles and fluence measurements.

WP - 3.3: Detectors for absolute and relative dosimetry (GAFchromic, CR39, Faraday cup, ...).

WP - 3.4: Radiobiology studies and measurements

Table 7.1 shows the scientific organisation of the proposal with the three research areas, the sub-working packages, the responsible and involved people. It have to be also underlined that the general layout of the ELIMED transport beam line, as it will appear at ELI-Beamlines in Prague, is already defined and divided into three different sections (Figure 5.1), we decided to divide our scientific activity in three WPs, each perfectly related to each section.

8 Link with other research Institutions and groups, research impact also respect the Horizon2020 program

The European ELIMED project prefigures multidisciplinary actions and, therefore, it implies the involvement of research groups belonging to different areas and different national and international institutions. The hardware implementation of innovative transport elements and dosimetric systems, the development of Monte Carlo applications for transport and treatment planning, and finally the testing of the whole apparatus and cells irradiation with the laser-driven proton beams must be accompanied by a close and fruitful collaboration of each WPs with other research institutions, that have already expressed interest and will contribute to different part of the project. In particular a huge part of the proposed experimental activity is planned to be accomplished in three different top-level laser facility where laser driven proton beams can be already produced (see the section 14). One is the facility hosted at the Queen's University of Belfast (UK) where the TARANIS laser system is available . The second one is the PALS facility, hosted by the FZU Academy of Science in Prague (CZ), where two different lasers are installed. Finally we will have the possibility to use the laser installed at the Korean GIST facility. The listed facility are strongly linked inside the ELIMED collaboration. Of course, we strongly hope in the future availability of proton beams at the Italian FLAME facility where protons with energy up to 30 MeV with thin targets and up to 60 MeV using structured targets could be produced. Part of measurement campaigns (Thomson spectrometer calibration, preliminary tests of the energy selector, characterization of the dosimetric systems), at least in the preliminary phase of the project, will be carried out at the CATANA facility (Hadrontherapy Centre and Advanced Nuclear Applications) at LNS-INFN in Catania. CATANA, which is a centre with a direct INFN involvement (one of the research units of the project), was the first proton centre in Italy, born from the collaboration among the Department of Physics, the Institute of Ophthalmology and Radiology of the University of Catania and INFN. The centre, specialized in the treatment of ocular melanomas with 62 MeV proton beams, provides a clinical proton beam, characterized in all its specific spatial, temporal and energy features. Access to this facility will allow characterization of the various hardware components that will constitute the ELIMED apparatus, as well as the check of the diagnostic and dosimetric

Table 7.1: Working packages, responsibilities and involved people of the ELIMED project.

Working package and corresponding scientific activity	Responsible	Sub-WP	Involved people
WP-1: Target, PIC simulations, plasma and laser-driven beams diagnostic	Dr A Anzalone	WP-1.1: Development and optimisation of targets for the proton productions. Quantitative evaluation of accelerated particles using Particle In Cell (PIC) simulations. WP - 1.2 Charged beams diagnostic: upgrade of INFN Thomson spectrometer for the diagnostic of charged beams up to 100 AMeV. IC, ICR, SiC and monocrystalline Diamond for TOF connections. Feasibility studies of a new Thomson spectrometer for beam energies up to 100 MeV. WP - 1.3 Optical and UV imaging and spectroscopy. WP - 1.4 X-spectroscopy and imaging.	A Anzalone, M Cutroneo, S Tudisco, G Turchetti M Sumini, S Cavallaro, GAP Cirrone, FP Romano, L Torrisi, F Musumeci, F Schillaci, A. Tramontana, L Pappalardo, A Scordino
WP-2. Energy selection system and beam transport	Dr M Maggiore	WP - 2.1 Feasibility studies of an innovative energy selection system and beam transport to transform the laser generated mixed beam in a clinical one. WP - 2.2 Monte Carlo simulations of the energy selection system. WP - 2.3 First prototype of an energy selection system up to 50 MeV.	M Maggiore, D Rifuggiato, F Romano, GAP Cirrone, L Calabretta, M Favetta
WP-3. Hadrontherapy transport, dosimetry and radiobiology	Dr F Romano	WP - 3.1 Evaluation of the coming-out beams dose distributions and of the secondary radiation generated inside the selection system. Design and Monte Carlo simulation of the beam transport line starting from the selection system and related radioprotection calculations. WP - 3.2 Development of innovative systems for in air diagnostic of accelerated particles and fluence measurements. WP - 3.3 Detectors for absolute and relative dosimetry (GAFchromic, CR39, Faraday cup, É). WP - 3.4 Radiobiology studies and measurements.	GAP Cirrone, M Musumarra, F Romano, L Raffaele, M renis, B Tomasello, G Malfa, L Manti, M Sumini, G Castellani, S Cavallaro, A Anzalone, A Scordino, A. Tramontana

systems.

As it appears evident reading this proposal, the role of the Geant4 Monte Carlo simulation tool is crucial in different aspects of the project. The scientific activity of the WP-3.1 is, indeed, based on the Geant4 simulations, which have an important role in the ELIMED project both for the beam line design and for the dose/fluence distributions foreseen in the planned experiments. Moreover, in a second phase, also radio protection assessments will be carried out by mean of Monte Carlo simulations. Some components of the ELIMED project are official members of the Geant4 International collaboration and actively contribute to its development. They have the opportunity to directly interact with other members of the international collaboration, through meetings with the heads of the various "working groups" related to the specific areas of development. Geant4 collaboration is composed by more than 100 researchers who constantly update and verify its components. It was born thanks to a Memorandum of Understanding (MoU) between all the institutions involved in the development and maintenance of the toolkit: CERN, ESA, KEK, SLAC, Triump, LEBEDV, LPNHE, ATLAS, BaBar, CMS, LHCb and INFN. Despite Geant4 has been designed at first for high energy physics, in recent years a huge activity has been undertaken concerning other fields of application, especially in medical physics. Many participants at the proposed ELIMED project are involved in the development of Geant4 applications related to the medical physics field. In particular they are strongly involved in the study of issues related to hadrontherapy, in the simulation of transport beam line for the therapy and in the development of algorithms for the evaluation of dose, LET (Linear Energy Transfer) and RBE (Relative Biological Effectiveness) distributions into biological material.

One of the main goals of the ELIMED project will be to improve as much as possible the international collaborations described above. This would permit to broaden the skills of the scientific community working in this field. In this last aspect we can find a clear link with one of the main goals of Horizon 2020 (Scientific excellence): the expansion and consolidation of excellence, in order to make European research and innovation more competitive. The proposed project would allow, in particular, the consolidation of partnerships between experts on the particles production and acceleration by lasers, on Geant4 applications development, on beam transport and on medical physics.

Finally, it should be stressed that the work toward the realization of the first hadrontherapy facility based on laser-driven beam (that will be the final goal after the preparatory phase of the next three years) could significantly improve the access of the future hadrontherapy treatments. Indeed, one of the main aspect which are boosting such a kind of application is represented by a relevant cost reduction and compactness which should characterize the future commercial lasers respect to the current hadrontherapy centre. If this two point were demonstrated in the next years, hadrontherapy could become a routinely treatment procedure of easy access, as can be considered today the photon radiation therapy. According to that, laser driven acceleration could represent an important step forward in the fight against cancer, which is one of the main causes of disability, early death and poor health conditions. Technological progresses in this direction certainly falls under the first goal of another priority of the Horizon 2020, that is, "Societal Challenges: health and demographic change".

9 Risk assessment of the proposed activity

A multi-disciplinary project, as ELIMED is going to be configured, is based by definition on the mutual interaction of different competencies and skills in order to fulfil specific goals. Therefore, in these cases, milestones are strictly related to each other and the attainment of a comprehensive objective depends on the fulfilment of the cross-related deliverables scheduled in the time plan. For such a kind of projects a risk assessment is necessary in order to preliminarily evaluate the key phases of the project and foresee the potential effect on the project time schedule. These assessments allow to plan in time the different strategies and the alternative solutions which should be followed to fulfil a specific milestone also in case a probable event risk takes place. Good rule is also to relate each risk assessment with a specific level of probability. The following Table summarizes risk assessments of each sub-WP, the effect on the project and the potential actions to be undertaken to overcome the issue with a minor impact in terms of time delay, cost increasing and lack of commitment:

Table 9.1: Risk assessments for the specific subWP: L = low, M = medium, H = high.

Owner	Risk	Probability	Impact	Effect of Project	If it happens: Actions
WP1.1	Difficult on optimization of thin nanostructered targets.	L	M	Changing in planned targets type to be used and, eventually, in the related diagnostic system.	Investigate other methods of optimizations. Identify alternative possibility of development (Prague group).
WP1.2	Issues for the upgrading of the Thomson spectrometer for the required energies.	L	M	Cost-increasing. Time delay.	Replacement of the spectrometer with a new one. Change of the measurements schedule.
WP1.3	Not clear assessments about plasma characterization coming from the use of a VIS and UV ICCD.	M	M	Change in strategy.	Change of the diagnostic method with an alternative one (X-ray spectroscopy).
WP1.4	Not clear assessments about plasma characterization coming from X-spectroscopy.	M	M	Change in strategy.	Change of the diagnostic method with an alternative one (Optical spectroscopy).
WP2.1	Technical issues in the realization of the energy selector according to the specific requirements.	L	H	Lack of commitment. Strong change in strategy. Closure of WP3 activity. Cost increasing.	Inform coordinator of WP3 and national responsible for the quick decisions. Commitment of an alternative system to an external farm.
WP2.2 WP3.1	Not reasonable results of Monte Carlo simulations	L	M	Change in strategy. Time delay.	Change of the Monte Carlo code used. Alternative analytical simulation for faster preliminary assessments.
WP3.2	Lack of accurate information on particle fluence detected by the innovative monitor system.	M	M	Failure to complete key task (dosimetry, radiobiology).	Investigate alternative system for proton fluence measurement: thin transmission foil or transmission ionization chambers (correction of saturation effects).
WP3.3	Big systematic errors in absolute dosimetry.	M	H	Failure to complete key task (radiobiology). Time delay. Change in strategy.	Investigate alternative detectors for dosimetry: calorimetry, TLD. Plan additional measurement campaign for further tests.
WP3.4	Not reasonable results for cellular response.	M	M	Time delay. Cost increasing.	Review of the considered assays in order to find coherent intercomparisons and/or new kind of response investigations. Increasing statics, if necessary.
WP1 WP2 WP3	Belfast TARANIS laser facility not available.	L	H	Time delay. Cost increasing.	Move to FLAME and/or Korea GIST laser facility or other laser facility.
WP1 WP2 WP3	FLAME laser facility not available.	M	M	Lack of some commitments.	Move to Korea GIST laser facility or other laser facility.

10 Physics background: particle production and acceleration by high power lasers

The investigation of fast ions emission from laser-plasma interaction is crucial for future applications of laser -accelerated ion beams in different areas, such as warm dense matter generation, probing of high electric and magnetic fields, probing of very dense matter, nuclear applications (compact neutron source, isotope production, fission reactions), medicine, astrophysics laboratory, new accelerator generation, etc..
The ion acceleration is due to the interaction of a high power (intensity $I > 10^8\ W/cm^2$) and sub-nanosecond pulse laser with solid target. The key in reaching such high powers is the chirped pulse amplification (CPA) technique, developed for radar devices more than 40 years ago. In the CPA scheme a pulse produced by a low power laser ables to create a really short packet ($\sim 50\ fs$) is first stretched in time (chirped in frequency) by a factor $\sim 10^4$, then amplified and finally recompressed. In CPA process not only an ultra-short high-intensity main pulse is produced, but also a weaker pedestal, or pre-pulse, due to the amplified part of the pulse that is not compressed again. The pedestal plays an important role in ions acceleration in fact even if its intensity is several order of magnitude smaller than the main pulse, it is enough to create a plasma [105, 106]. The electrons escaping from nuclei will acquire a kinetic energy greater than their rest mass, thus they become highly relativistic. In this context a useful parameter is the so called $laser\ strength\ parameter$, defined as:

$$a_0 = \frac{eA}{m_e c^2} \tag{10.1}$$

namely it is the peak value of the laser potential vector normalized with respect to the electron rest mass. It can be related to the peak intensity, I_0, and the wavelength, λL, of the laser by:

$$a_0 = \frac{e}{m_e c^2}\sqrt{I\lambda\frac{2}{\pi c}} \tag{10.2}$$

Thus, a_0 can be seen as the maximum momentum of an electron quivering in the laser field, normalized with respect to its rest mass, and the previous relation shows that relativistic regime is reached for laser intensity $I > 10^{18}\ W/cm^2$.
When an electromagnetic wave with optical or near infrared frequency ω is focused on a gas, the produced plasma has an electron density n_e less than critical density $n_c = me\omega^2/4\pi e^2$. Hence the plasma is called $underdense$ and the wave can propagate through it. This scenario allows electrons acceleration in the so called $Laser\ Wake-Field\ Acceleration$ regime.
Interaction with a solid target is radically different, in fact the electromagnetic wave promptly

ionizes the target forming an overdense plasma with $n_e > n_c$. The laser pulse can only penetrate in the skin layer $l_{sd} = c/\omega_p = (\lambda/2\pi)\sqrt{n_c/n_e}$ and the interaction is a surface interaction. In the interaction, part of laser light is reflected but a significant fraction of laser energy may be absorbed by the target.

For short laser pulses with relativistic intensity, plasma temperature rises very fast and the collisions in the plasma can be considered ineffective during the interaction. In this situation, different collisionless absorption mechanisms can arise, such as $resonance\ absorption$, $\mathbf{J} \wedge \mathbf{B}$ $heating$, $vacuum\ heating$ [107, 108]. In any case the absorbed energy will result in the heating of electrons fraction at temperature much higher than the initial bulk temperature. Laser energy absorption by electrons is a crucial phenomenon in ion acceleration. If normal incidence is considered, the ponderomotive force pushes inward the electrons from the rear surface of the target creating a charge separation which produces an electrostatic field experienced by ions. The first experiments exploiting the interaction of short ($\tau < 1\ ps$) and intense ($I\lambda^2 > 10^{18}\ W/cm^2$) laser pulses with thin solid foils, showed the production of proton beams in the range of several tens of MeV coming from the rear surface of the target.
In most experiments the dominant regime is the so called **Target Normal Sheath Acceleration** ($TNSA$) in which the accelerated protons come from the rear surface of the target and the accelerating field is due to the expansion of heated electrons around the target. In the interaction of an intense electromagnetic wave with a solid, the front surface of the target becomes ionized well ahead the pulse peak. The successive laser-plasma interaction heats the electrons via different absorption mechanism to high temperature ($T \simeq MeV$) and their free path becomes bigger than the plasma skin depth and than the target thickness. These hot electrons have a diffusive motion both in the laser direction and in the opposite one. Thus, they can propagate in the target reaching its rear surface where they expand into vacuum for several Debye lengths forming a cloud of relativistic electrons. The charge imbalance due to the cloud gives rise to an extremely intense ($TVolts/m$) longitudinal electric field, which is responsible for the efficient ion acceleration. The most effective acceleration mechanism takes place at the rear surface of the target where the high intensity electrostatic field can ionize the atoms present on the unperturbed surface and then accelerates the produced ions. The accelerated multi-MeV protons from the rear surface of the irradiated solid foil is achieved no matter its composition, because they come from the hydrogen rich contaminants present on the target surface, such as hydrocarbons or water vapor. The energy spectrum of the protons is typically exponential with a high cut-off in the range of tens MeV. Several theoretical models have been proposed in order to describe the TNSA regime, but the most efficient in predicting the energy cut-off and that gives also a good interpretation of the acceleration mechanism is the one proposed by Passoni at al. [109], despite the strong assumptions. A representation of

the electron expansion and ion acceleration from the rear surface of the target in TNSA regime is proposed in figure 10.1.

When laser intensities exceed $I = 10^{21}\ W/cm^2$, different regimes can be achieved. In these conditions the radiation pressure of the laser dominates on the heating process and the accelerated bunch is composed by ions coming from the irradiated surface of the target. These regimes are called $Radiation\ Pressure\ Acceleration$ (RPA) and the accelerating mechanism depends on the target thickness [110]. The bunches produced exhibit a remarkable collimation and a high energy cut-off; the maximum energy record of 58 MeV has not been beaten yet. On the other hand there have been significant improvement in the control of the beam quality and energy spectra which give the possibility to start feasibility studies on tumor therapy with laser-accelerated ions. Anyway, several studies are still required on the transport of the optically accelerated beams in order to delivery ions with suitable characteristics for clinical applications.

Within the ELIMED collaboration some experimental activities have been already performed

Figure 10.1: Schematic rapresentation of TNSA regime.

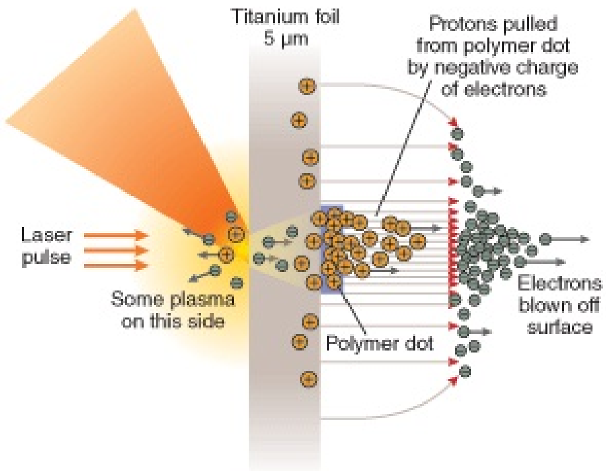

or scheduled at Prague PALS laboratory using the ion beams accelerated by the long pulse (400 ps), medium power (2 TW) infrared ASTERIX IV laser system.

Recently, the production of ions emitted with energy of few $AMeV$ and current densities of few A/cm^2 by the use of the sub-nanosecond, kJ-class lasers in the TNSA regime [6] has been proved [2, 3, 4, 5]. The dependence of ion maximum energy and current on the laser intensity have been investigated and apparently explained. Various parameters involved in laser-plasma ion acceleration mechanisms have been recognized in the last decade, however, the most of them have been investigated only partially and not fully explained. There are some reasons responsible for this situation which are related to some difficulties in the diagnostic techniques applied in the PALS measurements. It is evident that additional investigation are necessary to obtain more detailed characterisation of ion emission (measurement of angular distributions, individual ions intensity, dependence of ion emission on the type and structure of targets, etc.) and to find threshold conditions at which the mentioned nonlinear effects are starting to develop [7, 8]. The dependence of many plasma parameters (temperature, densities, gradients, electric fields, ion and charge state distributions,...) on the $(laser\ intensity) * (wavelength)^2$ (or $I \cdot \lambda^2$) factor permits to derive that the ion acceleration increases with the laser intensity (Figure 10.2). High energy laser pulses (1-1000 J) and short laser pulses (ps and fs lasers) may produce intense charge separation effects in plasma and develop high electric fields, inducting above $10 AMeV$ ions acceleration [9]. Many international laboratories are accelerating protons in the range of 10-50 MeV, exploiting the TNSA regime for laser intensity of the order of $10^{20} W/cm^2$ (laser facility Vulcan, Luli, Ral PW, Nova PW,...) [10].

Figure 10.2: Experimental data collection showing the scaling law ($I \cdot \lambda^2$ factor) for ion acceleration.

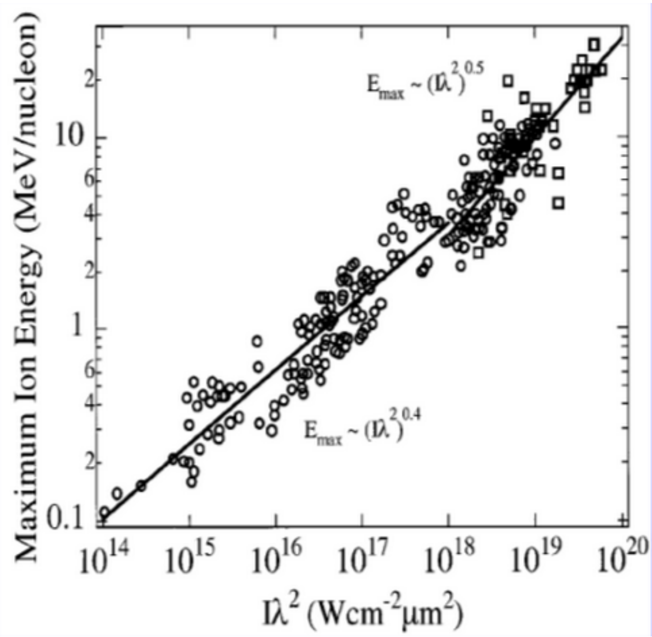

11 Detailed activity of the WP-1

11.1 WP-1.1: Particle In Cells (PIC) simulations and target studies

11.1.1 PIC simulations

The laser acceleration of protons has reached a sufficient maturity in the TNSA regime. It is based on electrons heating and subsequent creation of an electrostatic field due to charge separation. The protons inherit a Maxwellian spectrum and consequently it is exponential in energy with a cutoff proportional to the square root of intensity.

$$\frac{dN}{dE} = \frac{N_0}{E_0} \cdot e^{-\frac{E}{E_0}} \tag{11.1}$$

where E_0 is the average energy and N_0 is the total number of protons. The cutoff energy E_{max} is given by:

$$E_{max} \sim k \cdot a \tag{11.2}$$

with $a = 8.5 \cdot 10^{-10} \sqrt{I[W/cm^2]} \cdot \lambda[mm]$ and $k \sim 1-2$.

The average energy is typically $1/8$ the cutoff energy. Since the energy transferred to protons is a $1-5\%$ of the laser energy, close to the cutoff energy the number of protons is very low. At one half the cutoff energy (4 times the average energy) the number of protons is appreciable. Also the target thickness affects the maximum energy, in fact there is an optimum thickness close to the induced transparency:

$$a = \pi \cdot \sigma \tag{11.3}$$

where

$$\sigma = \frac{nl}{n_c \lambda} \tag{11.4}$$

With a=30, obtained with a 250 TW lasers, the cutoff energy can reach 60 MeV and at 30 MeV the number of protons is more than 10^8. In order to have a similar intensity at 60 MeV the power must be increased to 1 PW. The optimal thickness is quite low (a few hundred nm) and such targets are difficult to deal with. As a consequence, targets with a few microns coating of a foam with $n \sim n_c$ on the illuminated side have been proposed. The simulations confirm that these improvements increase the energy transfer to protons and their cutoff energy up to a factor of two. Finally an interesting regime occurs for targets having quasi critical density of a $50-100$ μm thickness (2-3 times the laser pulse length). The laser drills a hole creating at the exit a magnetic vortex and an electrostatic field which efficiently accelerates protons.

Simulations show that with a = 30 energies up to 100 MeV can be reached and this regime, known as MVA, is very robust unlikely the shock wave acceleration regime SWA. The full 3D simulations are carried out by Bologna researchers using the PIC code ALaDyn, its version for the GPU and the hybrid architectures Jasmine. The energy and spatial distributions obtained by simulations are suitable for the proton tracking along the transport line (collimators and focusing elements). Typically collimators and a high field solenoid can be used for focusing and energy selection. The ouput beam will have small size (a few mm) and small emittance (a few mm-mrad, it will be also suitable for injection into a RF cavity (eventual post-acceleration). The choice of the targets is crucial and we believe that at present solid targets with thickness slightly below 1 mm (improved TNSA regime) or low density targets (gas or liquid H jets) with thickness near 0.1 mm (MVA regime) offer the best opportunities for proton particle to reach 30 MeV or 60 MeV with adequate intensity for a = 30 and a = 60, obtained with a laser power of 250 TW and 1 PW respectively. Extensive 3D computations are required to guide the experiments. Extending the simulation range from a few hundred μm to a few mm or even a few cm allows to deal with the complex space charge and charge neutralisation effects due to the comoving electrons. The use of thin foils can reduce their number by one order of magnitude but their presence in the transport line needs probably to be taken into account. The space charge effects during beam transport need to be taken into account even though their treatment is not straightforward due the large energy spread. Figures 11.1 and 11.2 show two example of proton spectra obtained with the ALaDyn simulation code under different target condition as detailed in the caption.

Other regimes like Coulomb explosion or RPA promise higher energies and lower energy spread. However they are not well consolidated experimentally and much research work and targets development needs still to be performed.

11.1.2 Target preparation

Thick and thin targets will be prepared in order to control the plasma composition, ion and electron density. In order to increase the concentration of protons, hydrogenate targets will be employed, such as polymers (polyethylene, polystyrene, polymethylmethacrylate, mylar,....), hydrates (titanium hydrate and other metallic hydrates) and metals with absorbent hydrogen (gold, titanium, etc.). In order to increase the electron density for each target heavy metallic elements will be added, such as gold, as embedded nanostructures, nanospheres or as deposited thin films. Target will be prepared also taking into account the absorption coefficient of the laser wavelength. For this reason, special nano and microstructures will be embedded into polymers or deposited as thin films in multilayered structured foils. Carbon nanotubes and other nanostructures containing high hydrogen content will be employed to increase

Figure 11.1: Protons spectrum of a 3D simulation of a 0.5 μm solid target with a 2 μm foam layer at critical density for a=30 and a thin layer 0.05μm of contaminants. Average energy 7.4 MeV.

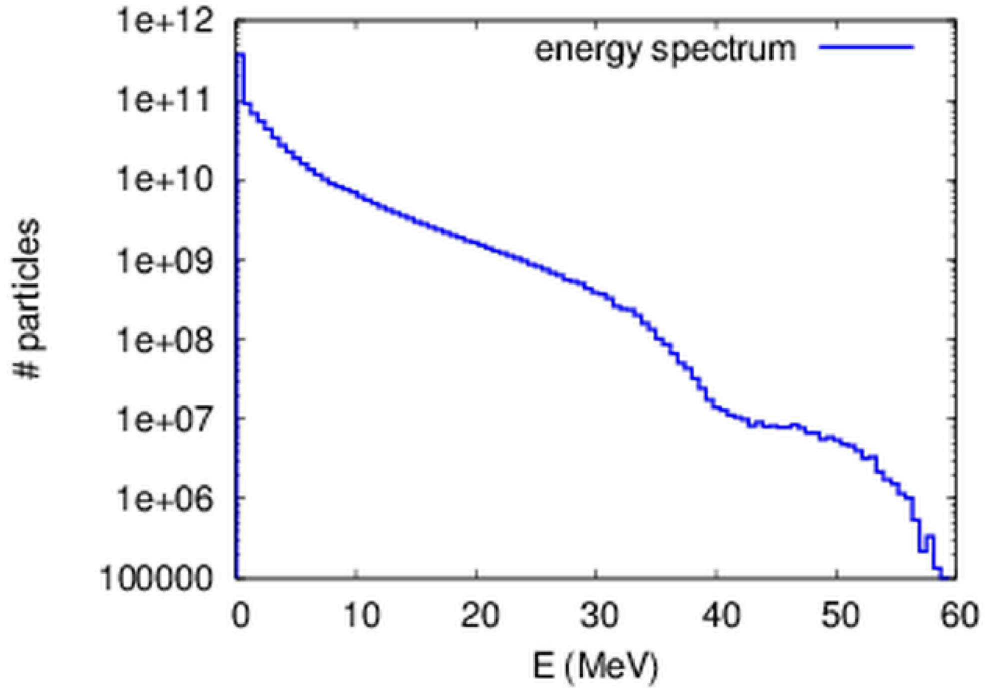

the absorption coefficient and the proton amount of the produced plasma. Proposed targets and foams will be employed to enhance the laser absorption and to decrease the reflection of the incident light so that the maximum laser pulse energy can be transferred to the plasma. A special attention will be dedicated to the preparation of thin foils, with a thickness below 10 microns, in order to be employed in experiments well described by TNSA approach that accelerate protons in forward direction. Different techniques, such as thin film deposition, sputtering deposition and spinning solution deposition, will be investigate to generate thin structured foils with thickness of the order of 1 micron. Resonant absorption effects will be also studied to generate non linear phenomena, for which p-polarized radiation can be absorbed at the critical density surface. Targets will be employed in different experiments in order to test their composition and thickness to obtain the maximum proton acceleration, according the Fuchs experiments (Figure 11.3).

Figure 11.2: Protons spectrum for a target of critical density of thickness 40 μm with a pulse having a=25 and P=150 TW . Acceleration in the MVA regime.

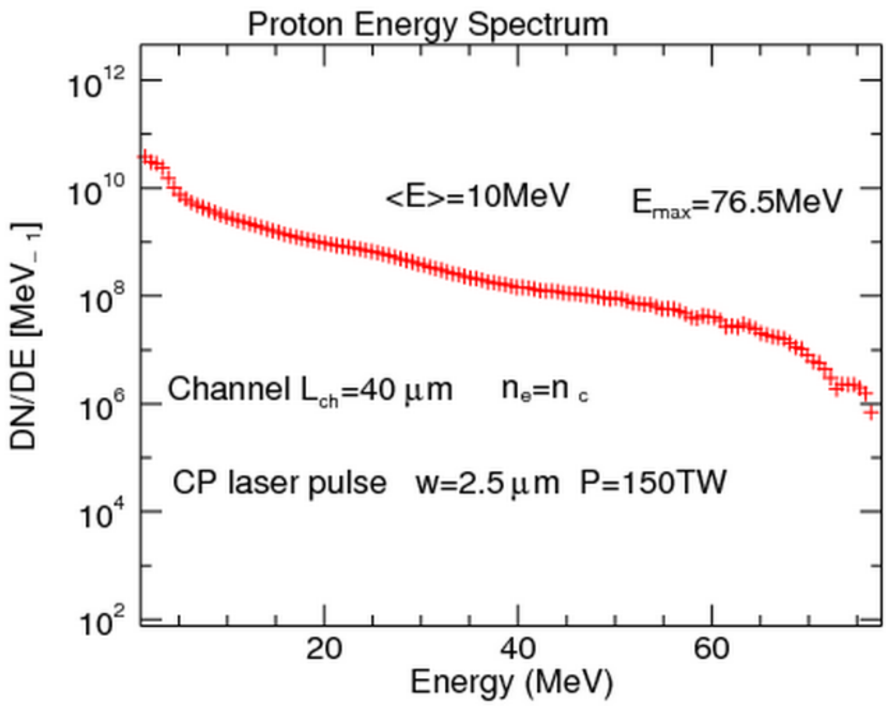

11.2 WP-1.2: CHARGED BEAMS DIAGNOSTIC

11.2.1 DIAGNOSTIC FOR LASER-DRIVEN IONS

Ion collectors (IC) and Ion collector ring (ICR) will be employed in time-of-flight (TOF) configuration in order to have immediate information on the average proton energy and yield in different angular directions with respect to the target surface normal directon. IC and ICR will be placed at different angles in forward and in backward directions and at different distances (higher than 1.5 meters) so that TOF measurements will permit to distinguish the photopeak on the collector, the proton contribution and the contribution of the slower ions coming from the other elements of the produced plasma. ICR will be employed in special manner in front of the Thomson parabola spectrometer in order to compare the maximum energy of the proton parabolas and the TOF evaluations. The IC and the ICR will be employed by using different sectors (generally four) equipped with different absorbers (generally thin Al absorbers from 1 microns to 8 microns in thickness) so that it will be possible to select very well proton peak from heavy ion peaks and from the photons producing photopeak. SiC (Silicon Carbide)

Figure 11.3: Maximum proton energy emitted by an Al target of different thickness

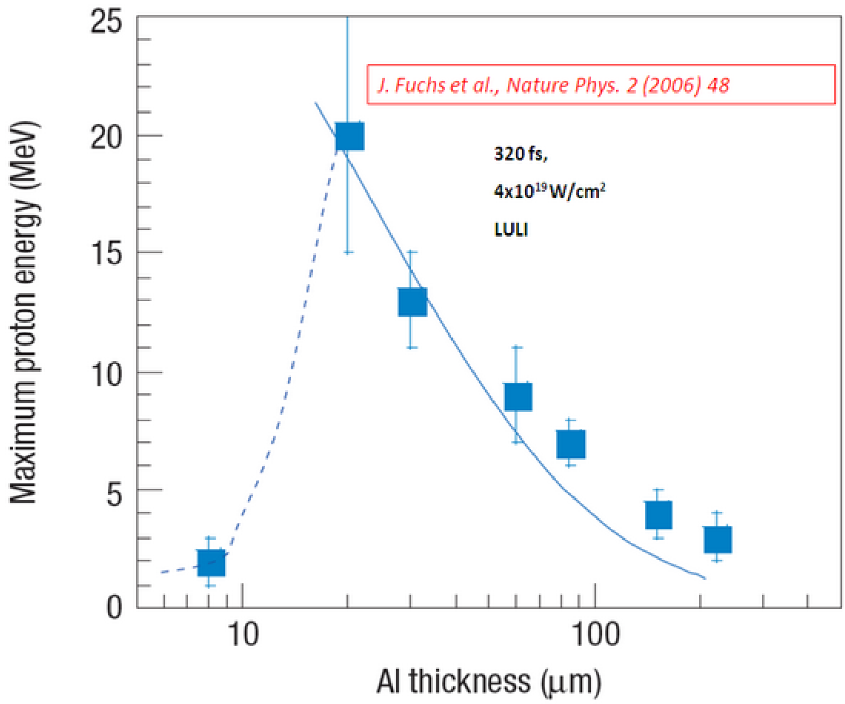

detectors will be employed because of their energetic gap (3.3 eV) which permits to detect no visible light but only UV and X-ray photons, and because of their high response velocity and high sensitivity. SiC will be employed in TOF configuration to reduce the background of proton peak and to highlight the proton contribution with respect to that of heavy ions coming from plasma. At ultra-intense laser experiments also monocristalline diamond detectors will be employed in TOF configuration in order to decrease the background due to the visible and soft UV to detect very well the proton peak and to measure their mean velocity and energy to be compared to the measurements with Thomson Parabola spectrometer. IC, ICR, SiC and diamonds will be placed at different angles in order to have information on the ion angular distributions as a function of the laser and of the target parameters. To achieve this goal, very fast storage oscilloscopes will be employed. Futher details on the use of these kind of detectors can be found in our literature [12, 11, 13].

Also electrons play a key role on protons acceleration mechanism **??** and the development of the related diagnostics can in future represent an important task in order to optimize the ELIMED beams that can be done with different detectors.

11.2.2 THOMSON PARABOLA SPECTROMETER

Thomson Parabola Spectrometer (TPS) is a widely and successfully used device for laser-driven beam diagnostic. It has the advantage of a quite simple working principle which allows to get a complete set of information in a single measurement [14, 15, 21, 17]. Within the INFN LILIA project an high resolution, wide acceptance Thomson-like spectrometer have been already developed at LNS [18, 19]. A scheme of the deflection sector with a simulated carbon ions beam passing through the device is shown in Figure 11.4.

Figure 11.4: Simulation of a carbon ions beam passing through the Thomson Parabola developed at LNS

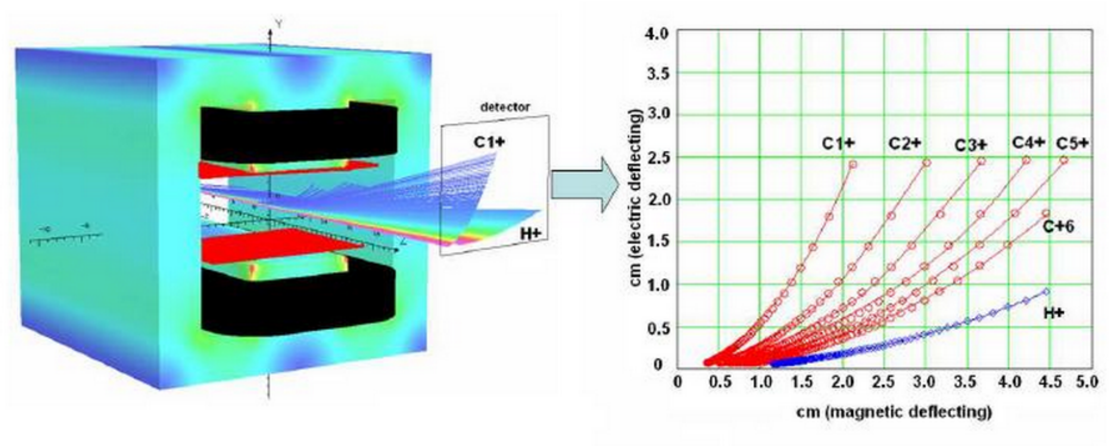

In view of the future ELIMED activity the TPS have been successfully tested at PALS laboratory in Prague, under ions beams accelerated with the ASTERIX IV laser system [20]. The acquired results have been analysed and compared against ICR time-of-flight information showing good agreement. Moreover another TPS developed at PALS and used since several years have been used during the experiment. Further comparison against the data acquired with the reliable PALS spectrometer have been performed successfully. Consistency among data shows the proper operation of the new Thomson Parabola as detector for beam diagnostic, even if some upgrades are still necessary in view to develop an improved spectrometer suitable for the higher energies expected within ELIMED project. Figure 11.5 shows a typical spectrogram obtained with a double-layer Mylar (2.5μm) and Al (50 nm) target, laser energy was 512 J.

The bright central halo is due to neutral particles streaming form laser-target interaction. It can be cause difficulties in evaluating the maximum energy of ions, as sometimes it overlaps with the starting point of parabolas. A new collimation system is required in order to reduce

Figure 11.5: Image of a tipical shot acquired with the Thomson Spectrometer of LNS. Parabolas of proton and carbonions with different charge states are visible.

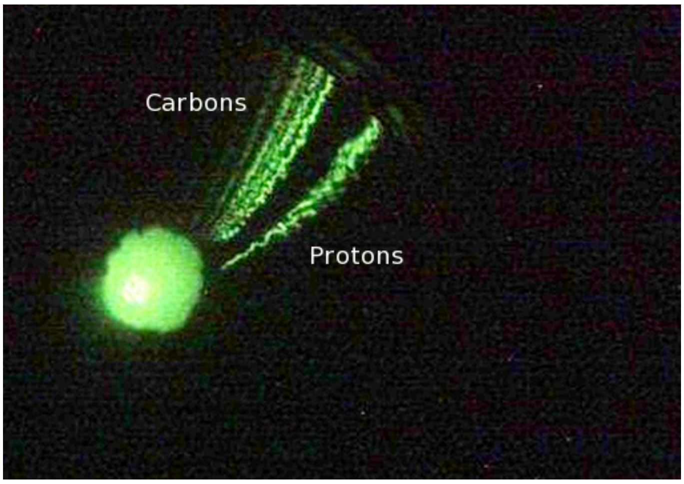

the halo dimensions. Moreover Al and O ions, elements in the target, are not resolved in spectrograms as their parabolas overlap with C ions traces. These issues can be resolved reducing the central halo dimensions and exploiting the whole MCP detector acceptance. In fact the minimum energy region, where parabolas are further from each other, is not visible on the active MCP surface. The main upgrade of the TPS concerns the improvement of the Field of View of the imaging detector. This can be done if all the ions reach the detector not along its axis. This would allow to exploit the whole detector acceptance making easier to resolve parabolas of different ions species.

The experimental phase has also shown some problems with the alignment and collimation systems. It should be possible to control the pinholes relative positions using a micro-metric screws system. This will permit to set the pinholes on the same axis and to control the beam spot position on the MCP detector. The possibility of using smaller pinholes, such as a system with 500μm and 50 μm in diameters, is also under consideration. This would allow to reduce the central halo dimension and to improve the spectrometer spatial resolution and its intrinsic energy resolution as well, as parabolas would be thinner and the energy range inside parabolas width would result smaller [21]. Finally, a pointing laser system ensuring the pinhole alignment and the alignment of the spectrometer with the interaction chamber have to be used. A micro-metric moving system is under testing, it will allow to fix the alignment laser position and set the spectrometer on the proper position with respect to the target in the interaction chamber. The upgraded spectrometer will be tested again at PALS laboratory during another beam shift that has been already approved for 2013. We hope in the possibility to test the system at the FLAME facility in Frascati within the end of 2013 or in 2014. During the same years the feasibility of a new Thomson spectrometer for proton energies up to 100 MeV will be performed. This study, based on the experience gained with the lower energy spectrometer, aims to realise the final spectrometer system to be used, as part of the diagnostic set-up, along the ELIMED beam line at ELI-Beamlines in Prague.

A specific *R*&*D* activity is also planned with the purpose to develop a new kind of imaging system for the spectrometer. We are evaluating the possibility to use plastic scintillator coupled with CCD camera as detector, to visualise the parabolic traces. A BC-408 scintillator, for example, can be used to resolve proton spectrum. Taking into account the overall resolution of the imaging system, we could obtain a minimum energy resolution of 100 keV. In order to verify the real possibility of this novel detection approach, we applied the physics evaluations given in [22] on the experimental data acquired during the experimental run at PALS in May 2012. We have calculated the number of protons per shot (9×10^7) entering the spectrometer, analysing ICR signals. Figure 11.6 below shows the estimated number of photons emitted by the scintillator for protons in the energy range 1.8-3 MeV (error bars are evaluated taking into account the solid angle of CCD lens, Quantum Efficency, etc. [22]).

Figure 11.6: Estimated number of photons emitted by the scintillator considering protons in the energy range 1.8-3 MeV.

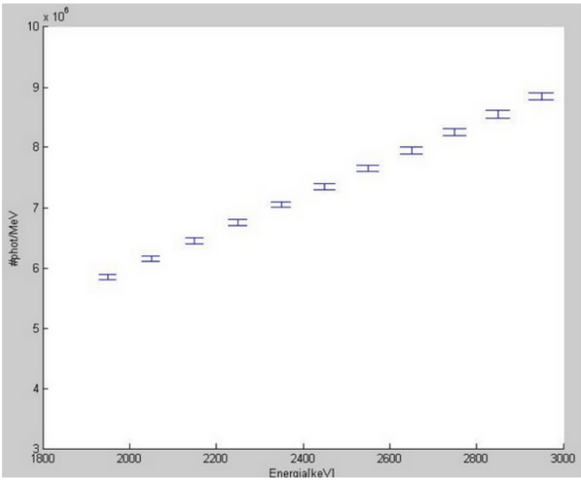

Starting from the experimental data we acquired, we have estimated the number of protons reaching the imaging system per energy slice of 100 keV, which is of the magnitude order of 10^6. Taking into account the CCD (14-bit CHROMA CX3 camera) QE and the scintillator emission spectrum (1 mm thick BC-408), we have estimated that at 2 MeV energy, a minimum of 10 protons are needed to be detected [22]. A scintillator-based ion beam profiler capable of measuring the ions beam transverse profile for a number of discrete energy range has been designed by Belfast researchers. It has been just tested and calibrated with conventional beams whose features are set similar to laser-generated beams ones. Preliminary results with non-conventional beams was obtained at RAL Laboratory, but many improvement of the detector are still necessary [2].

11.3 Optical and UV imaging and spectroscopy

The understanding of spatial and temporal distribution of plasma parameters in a laser-produced plasma is of great interest to many fields in science. As a matter of fact, between several techniques employed for diagnostics of a laser-created plasma, the photometric and imaging techniques can deeply contribute to plume investigation if they were able to provide a real time, two-dimensional information on the three-dimensional plume propagation [24, 25]. Indeed this capability is essential for hydrodynamic understanding of the plume propagation and reactive scattering. It gives information about the influence of the target nature and geometry on the plume characteristics. Since laser-produced plasma exist on sub-mm spatial and nanosecond temporal scales respectively, plasma diagnostics with these resolutions are needed. The advent of commercial intensified CCDs (ICCD), make it possible to obtain nanosecond time resolution, high spatial resolution and high sensitivity. Thus comprehensive and reliable information can be obtained even on electron density, electron temperature, plume species velocities and ionization balance. Recently [26] a laser plasma imaging technique has been reported. It permits simultaneous spatial, temporal and spectral analysis of the optical emission from laser-produced plasma plumes. The image of an expanding laser-produced plasma is focused on the entrance slit of a stigmatic spectrometer with time-resolved image readout. If the plume expansion axis is aligned with the slit, the obtained images are space resolved along the direction of expansion and spectrally resolved along the orthogonal axis.

Indeed this capability is essential for hydrodynamic understanding of the plume propagation and reactive scattering. Some preliminary experiments have been performed [27] obtaining the time resolved image of two colliding laser-produced expanding plasmas (see Figure 11.7).

Moreover, combining high time and spatial resolved optical spectroscopy with Langmuir probe measurements, the temporally and spatially resolved electron density and temperature at the stagnation layer were extracted (see Figure **??**).

In this proposal we want to use this novel technique to generate critically evaluated plasma parameters from the time resolved spectral images. It will be made by employing a getable ICCD camera sensitive from 185 up to 850 nm, with a pixel array of the order of 1024 x 1024, an active area of about 20 mm x 20 mm and a minimum optical gate width < 2ns. The laser system will be synchronized temporally with the main diagnostic systems using a delay generators

Figure 11.7: Time resolved imaging of broadband at different propagation times: 30 ns, t = 50 ns, t = 100 ns.

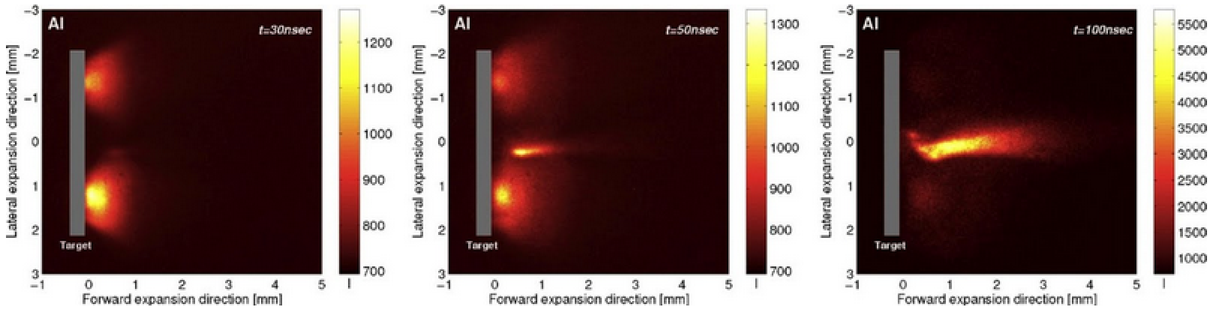

Figure 11.8: Electron density and electron temperature profiles vs. time for the seed and for the stagnation layer.

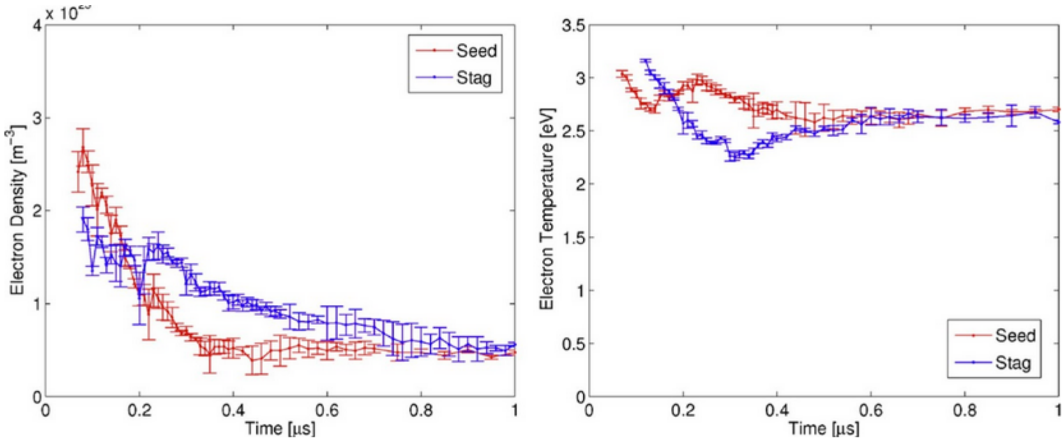

Fig. 2. Electron density and electron temperature profiles vs. time for the seed and for the stagnation layer.

with a maximum temporal jitter of 1 ns. A suitable optics based on zoom lens, together with an extension tube will allow to the ICCD to acquire highly magnified shots of the plasma. A suitable optical filter will protect the ICCD from any scattered laser radiation. Optical emission spectroscopy will be realized with two suitable imaging spectrograph, one for the UV and the other for the VIS range, with a resolution of 2 nm. The technique will be based on the approach of Siegel et al. described in [26]: the plasma focused on the entrance slit of the spectrograph produces at its output a one-dimensional spatial and spectral plume image. The vertical axis corresponds to its expansion direction (z) and the horizontal axis refers to the wavelength of the emission species. By placing the ICCD at the spectrograph output, will be possible to obtain simultaneously the spectral and spatial information of the plasma propagation; the temporal evolution will be then obtained by gating the ICCD camera.

11.4 X-RAY DIAGNOSTICS OF LASER PLASMAS: ENERGY-DISPERSIVE X-RAY SPECTROSCOPY, HIGH RESOLUTION X-RAY SPECTROSCOPY AND 2D SPACE-RESOLVED X-RAY IMAGING

The interest in using X-ray diagnostics for understanding the plasmas produced in laser-target interactions, have grown rapidly in the last decades [28, 29]. In fact the main self-emission from plasma lies in the X-ray domain. Thus, the analysis of the emission spectra (both the continuous bremsstrahlung and the line-spectrum resulting in transitions between bound levels of ionized atoms) can be considered a powerful tool for the non-intrusive investigation of the plasma matter. In particular, X-ray based techniques can be used to gain accurate information on electron temperatures, electronic densities and ionization states [28, 30]. The activity of the present sub-WP will be focused on the development and integration of analytical techniques based on the X-Ray Spectroscopy (both Energy-Dispersive and Wavelength-Dispersive) and X-ray Imaging to be applied in the investigation of the laser interactions with different target-material (i.e high Z and low Z atomic numbers) and target-structure (i.e. multi-layered, nano-structured, etc.). The main scope of the proposed diagnostics will be the investigation of the best experimental conditions for the final protons production (reproducibility, intensity and energy stability).

11.4.1 ENERGY-DISPERSIVE X-RAY SPECTROSCOPY (XRS)

Some of the participants to the ELIMED project have a strong experience in the application of Energy-Dispersive X-Ray Spectroscopy (ED-XRS). In past experiments a number of ED-XRS spectrometers where developed and tested with X-rays of different energies (from 1 keV up to 100-200 keV) emitted by microwave generated plasmas [31, 32]. In particular fast and high efficiency HPGe, and SDD detectors - all equipped with their own electronics and acquisition systems - are already available and will be used for studying the X-ray emissions of laser-plasmas in different energy domains. In particular, since laser interaction with target materials produces high-brilliance emissions (for examples in table-top lasers it is estimated to be about 1010-1012 $ph/sec/mm^2/mrad^2$ for metals) [2], measurements will be carried out using large active area (50-80 mm^2) SDD detectors that allow to operate with high counting rates (up to 500 KHz) and optimal energy resolution (133-138 eV at the reference value of 5.9 keV). Information on the electronic temperature can be extracted from the continuous component; also, X-ray lines emitted by atoms with different ionization state can be highlighted through the broadening of the characteristic peaks. Even if ED-XRS presents poor energy resolution in order to gain accurate information about plasma parameters, it represents a fast method in order to perform preliminary studies about the laser-target interactions. During the 1st year the participants will optimize the detection systems using microwave generated plasma sources already available at the LNS.

11.4.2 High Resolution X-ray Spectroscopy (HR-XRS)

The plasma parameters (i.e. electron temperature, density, charge states) can be accurately measured with the known methods based on the line intensity ratios and on the line broadening [28, 30]. It should be noted that the interaction of the laser with target produces exploding plasmas with atoms in different ionization states. Depending on the Z of the target, few atomic electrons (in H-like, He-like, Be-like, Li-like, etc., configurations) are produced. Such atoms in their own state of charge will undertake electronic transitions between bound levels and emits characteristic radiation. The latter results shifted with respect to the one measured in the neutral state. Also, satellite transitions can be efficiently excited. Thus, in order to approach the accurate measurement of line-shift and line-width, a spectrometer with a challenging spectral resolution (Dl/l=$10^{-3} - 10^{-4}$) should be developed. Moreover, such a system should be able to operate in a wide energy range in order to investigate different Z target. To satisfy the above requirements a HR-XRS spectrometer suitable for investigating a wide energy range with appropriate energy resolution will be developed . In particular the spectral evaluation will be performed by using 2 complementary line-space gratings (Bragg law based) operating from about 1.241 keV (1nm) down to about 60 eV (20 nm) coupled to a new CCD camera (back-illuminated CCD, 1024 × 1024 pixel, 13.3μm size, 16 bit, 5 MHz redout, $QE = 20\%$ at 10 eV, $QE = 95$ % at 1 keV). The spectrometer will operate under vacuum. During the 1st year of activity, we will take care about the acquisition of the instruments, we will develop the appropriate goniometric mechanics in order to select the opportune incident angles for the different energies to be investigated. Preliminary tests will be performed at the end of 2013.

11.4.3 2D X-ray imaging and spectroscopy

In the recent research activity of the UTOPIA experiment (5th Group of INFN) a X-ray pinhole camera have been developed and successfully applied in space-resolved imaging and spectroscopy of microwave generated plasma sources [33]. Such a system is particularly suitable to operate in the energy range between 1-30 keV, related to the hotter component of the plasmas (the Quantum Efficiency of the system is 85 % – 90 % in the region 1-10 keV). It consists of a CCD device containing 1024 × 1024 X-ray sensitive silicon pixel. Each pixel presents a 13.3mm size and it is back-illuminated in order to minimize the absorption of the lower energies. The CCD can be cooled down to a temperature of $-100°$C (under vacuum) with a strong reduction of the dark-signal (the associated noise is only 5×10^{-3} electrons/pixel/sec).

The CCD operates in Photon Counting mode, with a linear relationship between the number of photoelectrons generated by the X-rays incident in the camera and their energies ($N_{photoelectr.} = E(eV)/3.659$). Finally, the CDD camera is coupled to small aperture pinholes (in particular 5, 50, 75, 100 microns tungsten pinholes). The above experimental configuration allows to perform 2D spatial-resolved imaging and spectroscopy with a spatial-resolution up to 20 microns (mainly depending on the pinhole aperture, geometry and detected energies). During 2013 research activity will be focused to optimize geometry (pinhole apertures, source-pinhole and pinhole-CCD distances) in order to improve the spatial resolution and the magnification of the laser-plasma source with a typical dimension of $50-100\mu m$ (depending on the target typology). Moreover, the multi-filtered-pinholes method will be tested with known X-ray sources in order to acquire, in a single acquisition, the different spectral components composing the source. Finally, the use of external TTL coming from an ancillary detector (MCP) will be used as time gating (up to few ns) for the 2 CCDs.

12 Detailed activity of the WP-2

12.1 Beam selection and transport

The charged particle beams produced by the new techniques of acceleration by using the high power lasers, have interesting features: they are characterised by a very high peak currents ($10^{12}-10^{13}$ particles per shot, I > 500 mA) and both the transverse and longitudinal emittance are rather small. In fact, the transverse emittance, although it is characterised by very large angular width (up to 30 deg) gets a very small radial dimension depending on the size of laser interaction point on the target ($x100\mu m$). The result is a geometric emittance of order of < 0.1 $pi \cdot mm \cdot mrad$. With regard to the reduced longitudinal emittance, it is dependent on the very short temporal amplitude of the laser pulse (<1ps). The energy spectrum of the produced particles varies from a minimum of energy of few keV to the maximum value derived from the electric fields which are reached during the process of plasma expansion for the first instants of the interaction laser-target. Also the spatial distribution of the emitted particles on the target depends on the energy as shown in Figure 12.1.

So that these beams can be used in the context of the applications of the interdisciplinary physics [34] they must be characterized in energy and species and made of such size that they can be efficiently transferred to the apparatuses of measurement through the standard beamlines used for the transport of particle beams.

To do this, it is necessary to study the focusing techniques such as to maximise the number of particles transported and appropriately selected in energy and their relative spread [35].

Figure 12.1: The plot shows the strong angular divergence with energy dependent of the laser-driven beams.

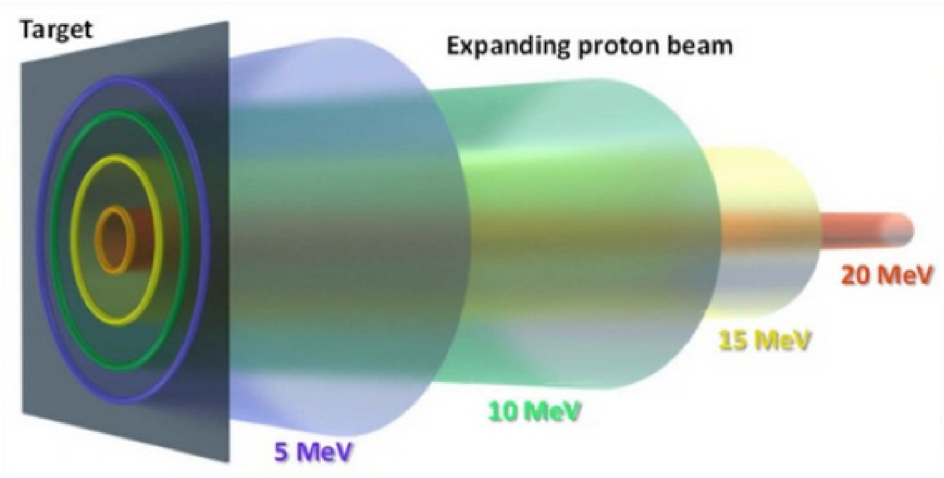

In general, the pattern of focus and selection of the beams produced in the laser-plasma interaction is characterized by the following steps (see Figure 12.2):

Figure 12.2: Steps into the pattern of focus and selection.

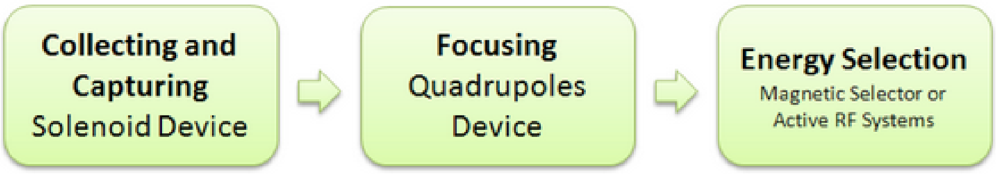

1. **Initial Phase of Capturing and Collecting:** it occurs nearby the point of production of charged particles. It aims to collect as many particles as possible and thus reducing the angular component of the transverse emittance. The device must be quite compact as it is necessary to place it inside the scattering chamber. This system provides the first coarse selection in beam energy. To do so, typically solenoid magnets are used, and pulsed high magnetic field [36]. In this first step is indispensable to carry out the beam dynamics simulations in presence of space charge effects due to the high current presence, but also the effects of the de-neutralization, namely the dynamics of electronic component in high intensity magnetic fields.

2. **Secondary Focusing:** It is done by means of the focusing devices which are positioned at the exit from the interaction chamber with the function of focusing on the transverse

direction the beam of particles pre-selected by the first phase of collecting. Since the system must be able to focus beams with different energies and with rather large transverse dimensions, it can be constituted by conventional electromagnetic or permanent based quadrupoles [37] with wide acceptance. The triplet configuration would ensure the focusing of particles in the two transverse space to a common point (waist). This would allow a subsequent focusing "point-to-point" of a possible conventional transport system. Also in this case a selection in energy by the above system is performed.

3. **Energy Selection and final beam characterisation**: the beam at the end of the second phase should produce rather small energy spread and transverse dimension (the first two steps help to reduce the transverse emittance by suppressing part of the beam), then the longitudinal emittance is also reduced. A magnetic system (consisting of a dipole or a series of dipoles in alternating gradient) can be used for final selection [96]. If the energy spread is relatively low and the energy is not excessively high, an active bunching system can also be used [39] to further reduces the spread in energy, keeping the number of particles transported.

12.2 Energy Selector Description

In order to select the energy of the particle beam produced by the target laser interaction, a magnetic system is under study. The device consists in four dipoles based on permanent magnets producing 0.7 Tesla each (see Figure 12.3). The second and the third magnetic fields are parallel with each other but oriented antiparallel to the first and the fourth ones. This configuration allows to increase the separation between the particle trajectories at different energy in correspondence of the central pair of magnets where, by means of a slit device, the particles with suitable energy are selected.

The energy spread and the amount of particles passing through the slit depends on the size of the aperture. The lower the energy spread, the lower the number of particles will be transported through the energy selector because it needs to use a smaller slit size and vice versa (see Figure 12.4). The energy of the proton beam can be tuned by moving transversely the slit position between 30 mm and 8 mm from the target normal axis. A roller guide system where the central twin magnets are placed, allows to displace radially the two magnets in order to increase the transversal displacement and select the lowest energy particles. In this way the energy could vary within the wide range of 5 MeV and 50 MeV. The energy spread reachable by using 1 mm slit aperture ranges from 3 % for low energy up to 30 % for the highest. The whole magnet system is almost 600 mm long and will be placed into the dedicated vacuum chamber. Two additional collimators are placed both upstream and downstream the selector system in

Figure 12.3: The figure shows the layout of the magnet system used as energy selector for the beam produced by the laser-target interaction.

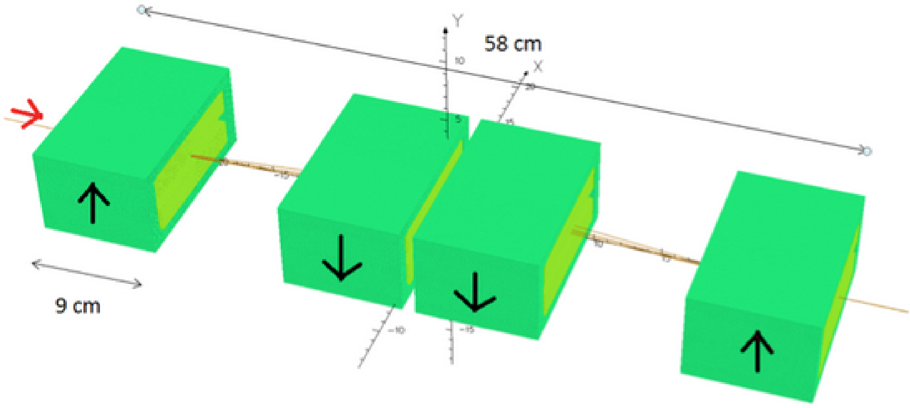

order to control the proton beam size.

The whole system will be simulated with the GEANT4 Monte Carlo toolkit in order to accurately predict the proton trajectories and energy spectrum of the selected beam. These information are crucial for preliminary calculations on proton fluence and dose per pulse. Moreover, the simulation will give also a quantitative estimation of radioactive activation produced by protons inside the energy selector, for further radio-protection assessments.

13 Detailed activity of the WP-3

13.1 Introduction

The WP3 is devoted to the study of feasibility of a proton in-air transport beam line for dosimetry and radiobiology studies. Different aspects have to be taken into account for such a kind of study, which involve theoretical calculations with simulations, as regards the part related to the project of the beam line, and experimental one, as regards development and test of detectors for diagnostic and measurements of dosimetry and radiobiology. Before clinical applications of laser acceleration becomes a realistic possibility, several tasks need to be fulfilled. The development of a dedicate therapeutic irradiation equipment, the transition from physical experiments with single shots of poor reproducibility to stable, reliable irradiation of patients with prescribed doses in a few minutes, addressing quality assurance and patient safety are necessary. Moreover, the real time physical and dosimetric characterisation and the investigation of the biological effectiveness are necessary. Thus, four different sub-WPs have

Figure 12.4: The plot shows the calculated energy spread as a function of the energy of the selected beam. The curves correspond to the values obtained by using two sizes of the used slit (0.5 and 1 mm).

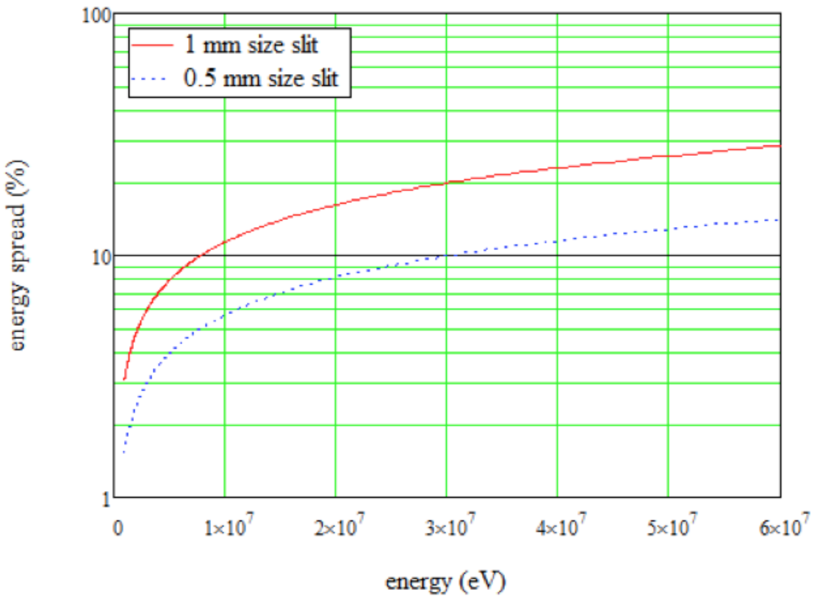

been considered, each one related to the mentioned aspects to be investigated

13.1.1 WP-3.1 Design and Monte Carlo simulation of the in-air transport beam line and radioprotection calculations.

This task is crucial for the design of the passive/active elements necessary for the in-air transport of the proton beams, once selected in energy. Depending on the collimation and on the spatial spread a customised system has to be simulated in order to obtain a "clinical beam" with the right requirements in terms of spatial homogeneity and symmetry. Monte Carlo simulations also permits to pre-calculate the environment dose in order to eventually design shielding elements for radioprotection. Moreover, the simulations of the experimental setup used in the laser facilities for the first test (Belfast, Corea, Flame) will be necessary to foresee dose per pulse and, according to that, reproduce the specific experimental configurations for the planned measurements.

13.1.2 WP-3.2 Development of innovative systems for in-air diagnostic of accelerated particles and fluence measurements

A dose-independent system is necessary for proton fluence measurements with the level of accuracy required for absolute dosimetry. An innovative system is proposed in order to overcome the limitations coming from the high currents per pulse and to perform in-beam diagnostic with a minimum beam perturbation.

13.1.3 WP-3.3 Detectors for absolute and relative dosimetry

Absolute and relative dosimetry for high pulsed proton beams is challenging because of the intense pulse dose involved. For this reason the study and characterisation of a set of dedicated detectors for dosimetry is necessary in order to select the most appropriate ones and to design a customised and integrated dosimetry system. Faraday cup, gafchromic films and CR39 will be tested in order to characterise their response respect to the dose rate and dose per pulse.

13.1.4 WP-3.4 Radiobiology studies and measurements

Despite there is a huge number of publications related to biological effects with hadron beams at conventional dose rate, the radiobiology at ultra-high dose rate with pulsed beams is almost unknown: only few experimental works have been published so far with laser accelerated proton beams. Moreover, most of them are focused only in survival fraction measurements, without deeply investigating the different involved effects. We propose to consider different end-points and study for each of them the effects of the ultra-pulsed beams with cells.

13.2 Activity on WP3.1

Evaluation of the coming-out beams dose distributions and of the secondary radiation generated inside the selection system; design and Monte Carlo simulation of the in-air transport beam line and radioprotection calculations with Monte Carlo (MC) simulations are today widely used in different fields. In particular MC codes for physical transport of particles in the matter are largely employed for medical applications because of the high level of accuracy of their predictions, also in very complex configurations. They, indeed, represent a fundamental tool for the study of dosimetric systems, the reproduction of clinical beam lines, the development and test of novel detectors and the verification of the Treatment Planning Systems (TPS). In this proposal we aim to use the MC simulation toolkit GEANT4 (GEometry ANd Tracking) to accurately reproduce the transport of the pulsed proton beam and to foresee all the physical quantities of interest. GEANT4 is one of the most versatile and widespread codes used today for particle tracking and it is widely used for different physical applications. It is a C++ object oriented toolkit permitting the simulation of particle interactions with matter [40, 41, 42]. It provides advanced functionalities for all the typical domains of detector simulation: geometry and material modelling, description of particle properties, physical processes, tracking, event and run management, user interface and visualisation. Initially developed for High Energy Experiments (HEP) simulation, GEANT4 is now widely used also for medical physics application. It allows, indeed, the tracking of any charged and uncharged particle relevant for radio diagnostics and radiation therapy. Some components of the LNS group involved in this proposal are expert users of this MC code and are member of the official GEANT4 collaboration since several years. We are also responsible of an application, currently distributed in the public release of the code, which simulate the CATANA proton therapy facility at LNS-INFN of Catania [43, 44, 45]. In the CATANA facility eye tumours are treated with 62 MeV proton beams [63]. The passive beam line is simulated in details with GEANT4, with the possibility of retrieve depth and lateral dose distributions as well as averaged LET of both primary and secondary particles. Our aim is to gather the LNS expertise in MC simulations in order to fulfil the followings scopes:

- MC simulations of the experimental setups to be used in the laser facility for the planned experimental activity (Belfast, Korea, Flame). The preliminary information retrieved by these calculations are important for the optimization of the experimental setup and a prediction of fluence per pulse expected at the measurement point. Accurate dose estimation will be done in order to foresee the response of the different detectors to be used (WP3.3).

- MC simulation of the energy selector (WP2.2). A realistic reproduction of the system and of the particle transport in the magnetic field allows an accurate prediction of the beam characteristics at the exit window and, consequently, to retrieve the expected energy spectrum.

- Feasibility study of the ELIMED beam line. An accurate simulation of the active/passive elements of the in air transport beam line will be done at the end of the project. The MC simulation will allow to study the best solutions for the spatial shaping of the beam, the homogeneity, the dose delivery system, the collimators and each kind of elements necessary to achieve a "clinical beam".

- Radio-protection studies. The full simulation of the transport beam line, starting from the energy selector to the in-air measurement point, will permits to predict the radiation due to secondary particles and to preliminary identify areas at high level of activation. This study will be helpful for eventual design of shielding elements.

13.3 ACTIVITY ON WP3.2

Innovative system for on-line diagnostic and relative dosimetry of laser-driven ion beams

In-beam diagnostic for the intense pulsed proton beam in progress at the ELI facility is a demanding task. Beam specification, as sketched in the ELIMED draft, reports a proton burst duration Dt=0.1-1 ns with pulsed intensity ranging from 10^{10} to 10^{12} p/burst. In addition it is mandatory to perform an on-line monitoring (negligible beam perturbation) and the detection system must operate in an EM polluted environment. An integrating or fast current transformer (e.g. Toroid) would represent a preliminary choice, since they are world-wide used and commercially available [47], but its reliability could be compromised by EM pollution. In order to match such "tricky" requirements an innovative, still simple, detection setup must be put in place. Simplicity and consequently reliability result as fundamental requirements for such a new diagnostic system. By using the experience developed at INFN-LNS and ISOLDE-CERN [48] and considering the constraints dictated by the beam specifications we propose a proof of concept to be validated. Introducing the ELImon, a compact and scalable in-beam monitor for pulsed beam. The detection system is described in the figure 13.1.

Pulsed beam will be diffused by a thin Au target (on-line monitoring), the elastically scattered protons will be detected at a tunable angle (in order to change the intensity range) by a battery-powered detection system consisting of a plastic scintillator coupled to a PM. Such a detector will work in full pile-up mode (total charge to pulse height conversion), allowing a simple and linear intensity-to-pulse height conversion. In such a way downscaling of beam intensity will be performed by the elastic scattering, intensity measurement by pile-up summing. A hand-held low-power MCA system will convert each pulse, the histogram will be stored in the internal MCA memory and will show intensity distribution over several beam bursts. The intensity profile will be download via optical link during the inter burst time interval, defeating the strong in-burst EM noise. The set-up geometry is well adapted for beam alignment monitoring too, just by using two or more symmetric modules around the Au target. Due to the simplicity of the set-up we will be ready to test a first prototype at the beginning of 2013.

13.4 ACTIVITY ON WP3.3

Figure 13.1: Layout of the proposed new detector for the on-line monitoring of the pulsed beam fluence

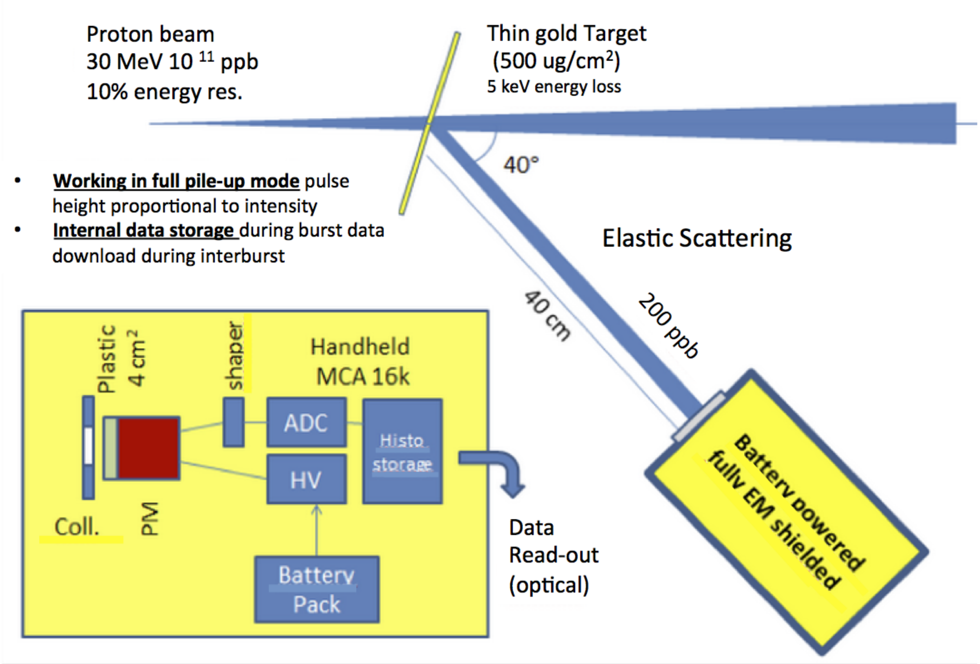

13.4.1 Introduction: Detectors for absolute and relative dosimetry

Due to the broad exponentially shaped energy spectrum, the low-energy range of the protons up to now available in the laser facilities and the high pulse dose, the dosimetry for this beam quality is challenging. Thus, an independent absolute dosimetry and online relative dose monitoring system are crucial prerequisites for successful radiobiological and clinical experiments with laser-accelerated protons. Integrated systems have been already developed for such a kind of application [49]. We propose to develop and test different detectors for dosimetry and to design a more general integrated system for dosimetrical measurements and cell irradiation. In particular we aim to use radiochromic films (RCF) and CR39 for relative dosimetry and to develop a dedicated Faraday cup (FC) for dose rate independent absolute dose measurements. RCF and CR39 can be used in stacks in order to achieve quantitative information on the energy spectrum of a specific bunch of accelerated protons [68, 82, 52, 53, 55]. An accurate measurement of the energy spectrum is fundamental for a precise calibration of the FC. Moreover the high spatial resolution of the gafchromic films allows a precise measurement of 2-D dose distributions at different depth, which is crucial for the cell irradiation. The characterization of these detectors with pulsed beams and the realization of an integrated system of absolute dosimetry in combination with a relative on line dose monitoring are a key requirement for in vitro cell irradiation and, therefore, for eventual future in vivo irradiation studies.

13.4.2 Radiochromic films

Radiochromic films, showing small energy dependence, high spatial resolution (up to 50μm) and tissue-equivalence, are a preferable media for ionizing radiation dosimetry measurements in clinical radiation oncology [57]. The radiation sensitivity is based on a solid solution of colourless crystalline diactylene monomer (sensitive component) coated on a flexible film base; when the active component is exposed to radiation, it reacts to form a blue colored polymer (self-developing films), with the possibility of handling in visible light. Figure 13.2 depicts the absorption spectra of a gafchromic film before and after irradiation. Before irradiation the active component produces little response as highlighted by the low absorbance at 636 nm. The change in optical density following dose deposition in gafchromic films may be measured with transmission densitometers, film scanners or spectrophotometers; a simple readout of the irradiated film can be obtained by using flatbed RGB scanners in the red channel [58].

Figure 13.2: Example of absorption spectra of an EBT3 gafchromic film before and after an exposure of 2 Gy of photon irradiation.

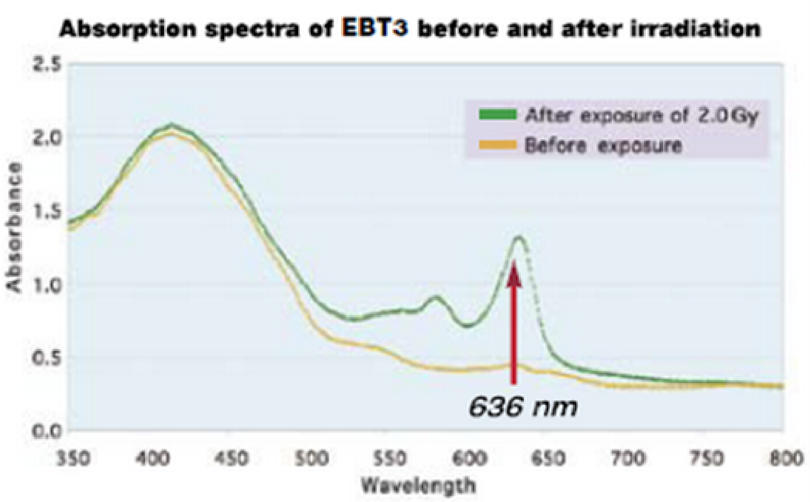

The RCF are presently widely used for absorbed dose measurements of high-energy photon beams produced by medical linear accelerators, including IMRT therapy and IORT [59].

Different models of RCF are available, with different dose sensitivity to be used in different dose ranges and different depths of the sensitive component:

1. **Gafchromic HD-V2**, dimensions 8 ×10 inches, dose range applicability 10 Gy - 1000 Gy; its Equivalent depth in water, Effective point of measurement, is 4μm; the Effective atomic number is 6.5.

   The Gafchromic HD-V2 high-dose dosimetry film has been designed for the use with beams of photons, electrons, protons, ions and neutrons. Its sensitivity is very low for clinical applications, but its effective point of measurement is at a depth of 4 microns and represents the shallowest point we were able to establish with radiochromic films.

2. **Gafchromic MD-V3**, dimensions 5× 5 inches, dose range applicability 1 Gy - 100 Gy; its Equivalent depth in water, Effective point of measurement, is at 125μm; the Effective atomic number is 6.7.

   As INFN-LNS Catana team we have investigated the above mentioned films with proton beams of the eye proton therapy facility in the energy range from 20 to 62 MeV. MD films have been characterized at LNS-INFN with a low energy proton beam of 21.5 MeV directly in a water phantom [60]. The films have been used also for the commissioning of Catana eye protontherapy facility [61, 62]. Moreover, they are currently used for routinely dosimetry measurements for the characterization of the clinical proton beam [63, 64].

3. **Gafchromic EBT3**, dimensions 8×10 inches, dose range applicability 1 cGy - 40 Gy; its Equivalent depth in water, Effective point of measurement, is 140 μm; the Effective atomic number is 6.98, very close to water (7.30).

   The GAFCHROMIC EBT3 dosimetry film has been developed specifically for applications in conventional radiotherapy. The response of EBT3 films to medical ion beams has been extensively investigated by many authors for the use in protontherapy and carbon ion facilities, as passive and active facilities, resulting in effectiveness of radiochromic films for absolute and relative dosimetry. The EBT film response was found comparable for protons and photons. From the acquired experience, EBT films are at the moment extensively used at passive proton-therapy facilities for lateral beam profile measurements in clinical beams of different proton energies and for measurement of unmodulated and modulated (clinical) depth dose curves. EBT films are used also for the commissioning of the pencil beams in hadrontherapy facilities with active scanning beam delivery (p,^{12}C) [65, 66, 67, 68].

   In ocular proton therapy EBT3 films are routinely used for beam profile measurements in unmodulated and modulated beams, including accurate determination of lateral penumbra, for the determination of output factor in the narrow beams of eye protontherapy and for 2D dosimetry. EBT calibration is carried out with 62 MeV mono-energetic proton beams, using a 25 mm diameter circular collimator. Several $3 \times 3cm^2$ strips are irradiated in a solid water phantom at 1mm depth in the entrance plateau of the Bragg curve, corresponding to a dose rate of 25 Gy/min. Calibration curve is well in agreement with the corresponding curve for 6 MeV photons (Figure 13.3), demonstrating the water equivalence of EBT film.

Figure 13.3: Curve calibrations of the EBT3 Gafchromic detectors irradiated with proton and photon beams.

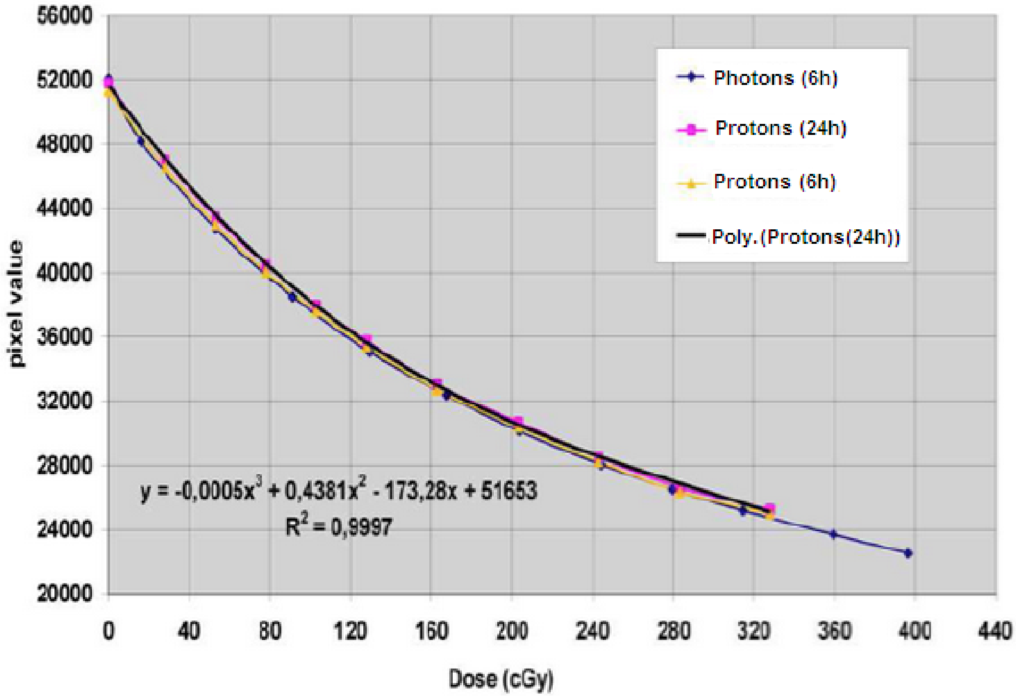

EBT has minimal dependence of response (< 2%) upon the residual range beyond the irradiation depths in the interval of residual ranges from 6 mm (25 MeV) to 30 mm (60 MeV); as a consequence, only one calibration file is required to obtain off-axis beam profiles at different depths in SOBPs. In this project we aim to gather the LNS expertise in dosimetry with RCF in order to use them for the followings scopes:

- as a relative dosimeter to be calibrated against an absolute one
- for dose measurements to measure 2D spatial dose distributions in stack configuration to perform laser driven proton beams spectroscopy.

Moreover, recent experimental studies show their dose-rate independence (< 5%) also for high peak dose rate of the order of 10^{10} Gy/s, typical of laser-based acceleration [69].

13.4.3 CR39 DETECTORS

The SSNTD (Solid State Nuclear Track Detector) CR-39 is a polycarbonate plastic largely used as detector of protons and heavy ions [70]. A particle impinging on it produces a molecular damage in the cylindrical region of the crossed material. This region extends for few tens of nano-meters along the particle trajectory. It is the so-called LT (Latent Track). REL (Restricted Energy loss) is instead the energy lost by particle to form the LT. A chemical etching transforms these damaged trails into permanent structures called ion track.

The detection sensitivity s of a CR-39 detector is defined as:

$$s = \frac{v_t}{v_b} \tag{13.1}$$

where v_t = track etch rate and v_b = bulk etch rate
This detector response is proportional to $\left(\frac{dE}{dx}\right)_{REL}$, namely to the loss of energy to form the LT.
Note that v_t is greater of v_b and therefore s is greater of one. The etch rate v (either v_t as v_b) is a function of etchant temperature and concentration [71].

Several authors have performed tests of sensitivity at low energies with different ions.

With regard to the protons we have:

50 KeV   L = 0.19 ± 0.05 μm
100 KeV   L = 0.40 ± 0.06 μm
200 KeV   L = 0.41 ± 0.04 μm

where L is the length of the particles trace measured after etching [70].
On the other hand, for higher energies (order of Mev) protons the range L is of the order of a few hundred microns (150 μm at 3.5 MeV) [72].

CR39s do not detect electrons and electromagnetic radiation, hence they can be used, together with ion collectors (IC) and RCFs, for detecting energetic protons produced by ultra-intense laser [73]. In these experiments we have bunch of protons greater than $10^8\ cm^{-2}$. Therefore, Al foils ($> 0.65\mu m$) have to cover the CR39 detectors in order to avoid overlapping of proton craters. This way, the low energy component of proton flux is absorbed in the foil and only the higher energy part of the bunch reaches the detector, allowing better crater separation. In such a way it is possible to estimate the flux of protons as a function of its energy [72].

Figure 13.4: Photos of craters induced in the CR39 by protons which were generated by one laser shot and penetrated through Al-foils of different thickness [72].

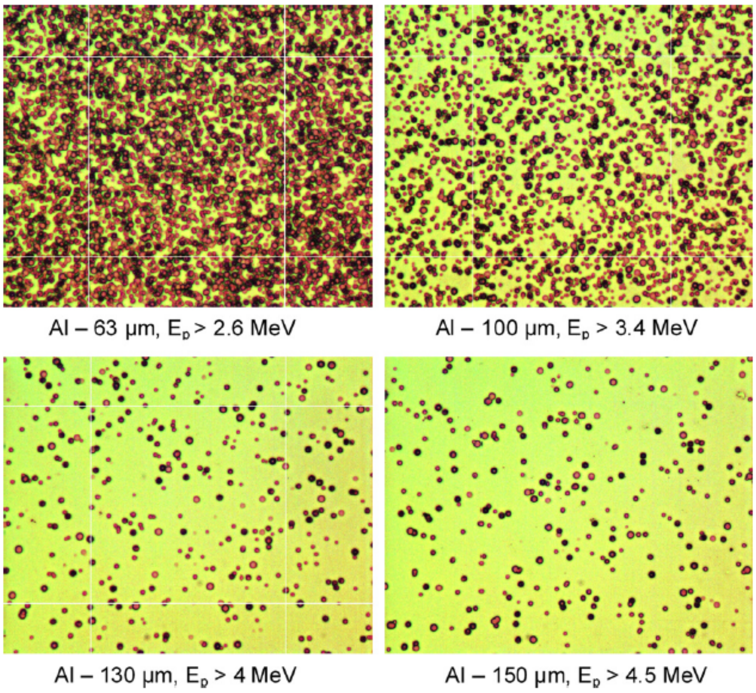

At LNS we have worked with this detector type in several experiments to detect alfa particles from nuclear reaction ^{11}B+ p present in a plasma formed after interaction of a laser pulse with solid target containing natural B [74]. We have done the calibrations with both alpha sources that with proton beams at several energies. We have a chemical batch and a motorized microscope controlled by a LabVIEW based software developed by our group, for the readout of the tracks. The analysis of the tracks was done by means of *ImageJ*, a public domain Java image processing software [75].

13.4.4 FARADAY CUP

A procedure to develop a calibration method for absolute dose evaluation have to be implemented as no protocol for absolute dosimetry with laser-driven beams has been defined up to now. In TRS-398, it is suggested that the charge collection efficiency in an ionization chamber should be assessed by a dose rate independent system such as a calorimeter. Since a Faraday Cup (FC) can perform absolute dose measures, as it has a linear response with the given number of particles and it has a signal which is independent of the dose rate [76], it can also be used for this purpose. Under certain circumstances, when the energy spectrum of the beam and the particle fluence distribution are known, an FC can also be used to determine the absorbed dose [77]. Absolute dose measurement with a Faraday Cup is possible using the expression:

$$D_w(z) = \Phi \cdot \frac{S_w(z)}{\rho_w} \cdot \prod k_i \tag{13.2}$$

where $S_w(z)$ is the stopping power of the proton spectrum at depth z and $\prod k_i$ is the product of the correction factors for beam divergence, scatter, field nonuniformity, beam contamination and secondary particle build-up. Is is obvious that this method relies on accurate value of the proton stopping power in water for which the uncertainty is estimated to be 1-2 % according to ICRU Report49 [78].

The previous equation, in the concrete implementation, can be written as:

$$D_w = \frac{1}{A(\frac{S(E)}{\rho})_w} \cdot \frac{Q}{e} \cdot 1.602\ 10^{-10}\ \ Gy \tag{13.3}$$

where A is the effective beam area in cm^2, $(\frac{S(E)}{\rho})_w$ is the mean stopping power in water in $MeV cm^2 g^{-1}$ at the considered proton energy E, Q is the total charge transported by the beam in Coulomb, e is the elementary charge in coulomb. For the experimental proton beam the stopping power in water is $\frac{S(E)}{\rho} = 10.516 MeV \cdot cm^2 g^{-1}$. Elastic nuclear interactions are also included: their ratio to the electronic stopping power is about 0.3 %.

In our case, even if the real applicability of an ionization chamber has to be verified and it is not obvious, Faraday Cup (FC) dosimetry will be implemented in connection with other dosimetric system (like Gafchromic and CR39 plates) to perform a preliminary real-time dose measurement. The laser-driven protons field size can be verified by using a fluorescence screen and a CCD camera [79] or with a detector scanner using

Gafchromic films. Inside the ELIMED activity we propose to develop a specific FC to be used for absolute dosimetric measures and to be physically connected with the energy selector system. The FC design will be based on a typical FC for proton beams like the one developed in [80]. It will work under vacuum and it will be movable to permit the positioning of other detectors (CR39, Gafchromic) and cell samples. The device will be developed in 2013 and in the same year we plan to perform the first dosimetric tests with conventional proton beams available at the INFN-LNS, in a large dose-rate range (1 - 500 Gy/min). In 2014 we plan to perform the first characterisations of this device with the laser-driven beams at the TARANIS facility in Belfast. In 2014 the integration of the system with the selection device will be also performed and final characterization of the device will be carried out in 2015 at the GIST (Korean) or FLAME (Italian) facilty.

13.5 Activity on WP3.4: Radiobiology studies and measurements

13.5.1 Rationale and state of the art

The possibility of using high-energy laser-driven charged particles for medical application in the near future opens a new and exciting scenario but also poses tremendous technical challenges. Before any clinical phase can start and aside from obstacles which nowadays exist for the generation of stable, sufficiently energetic and controllable laser-driven charged beams, two important issues need to be addressed thoroughly: dosimetry, as above illustrated, and radiobiology. As far as the latter is concerned, the development of such laser-driven ion beam sources will result in the generation of highly pulsed beams, the operational dose rates will be orders of magnitude greater than those presently used in proton or carbon-ion cancer treatment. However, the biological response of cellular systems to ultra-short pulses at variable pulse frequency is essentially undetermined and validation of the temporal aspects of the irradiation with regard to the biologically relevant response needs to be performed before they can be safely implemented in clinical routine. We shall therefore aim at optimized techniques and experimental procedures in order to measure possible differences in terms of biological effects between such high-pulse and very high-dose rate beams and those used conventionally. To achieve this, our strategy will focus on three major radiobiological endpoints: cell survival, which still represents the golden standard against which any radiotherapy-directed application must compare, DNA damage, as assayed by the comet assay and immunofluorescent detection of phosphorylated gamma H2AX (gamma-H2AX), and cellular premature senescence, which is a sublethal stress response of potential long-term impact on normal tissue homeostasis and organ functionality.

Several groups around the world have already started preliminary investigation on the methodology and possibility of using laser driven ion sources for cell irradiation experiments [81, 82, 83]. The radiation-induced cellular response is indeed determined by the rate at which the dose is delivered, in addition to the total administered dose and the phase of the cell cycle in which the cell is located at the time of irradiation. Furthermore, the observed effects will depend on the analysis time post-irradiation due to the speed of some cellular processes that may either amplify (i.e. radical species diffusion, in the order of psec) or reduce them (i.e. repair mechanisms ~ sec to hours). Dose-rate effects are well documented when irradiation regimes typically at Gy/min are lowered towards chronic exposure conditions (i.e. down to cGy/s). On the other hand, there is a very small knowledge of the effects at higher rates. Moreover, experimental evidences to date on the radiobiological properties of these irradiation conditions are limited and mainly using low energy (up to 20 MeV) proton beams or IORT electron beams [84, 85, 86, 87, 88, 89].

Early studies also investigated the effects of very high dose rates (in the order of 10^{11} Gy/min) on mammalian cell survival: an apparent lower effectiveness was reported for x-rays administered in the form of very short impulses (7 ns) and found that the cell survival curve resembled that observed under anoxic conditions [90]. Early animal studies also showed an effect, albeit in the opposite direction, i.e. towards an increase in radiosensitivity of intestinal epithelium when the dose rate increased from 1 to 60 Gy/min [91]. However, using electron beams at much higher rates (10^3 to 10^9 Gy/min), Field and Bewley [92] using 7 MeV electrons and Inada et al. [93] using 8 MeV electrons on mouse and rat skin found a decreased effectiveness compared to conventional regimes. In these studies, the decrease in radiation effectiveness was attributed to oxygen depletion under regimes of ultra-high dose rates since experiments done on skin under hypoxic consitions did not show similar behaviour. In other words, normal cells that are at low oxygen tension may potentially become anoxic at high doses delivered at high rates.This is in agreement with the observation that, at high dose rates, dissolved gaseous oxygen in cells may be depleted which would render the cells more radioresistent [94]. Indeed, some of the more recent results obtained with IORT electron beams by our group [84] point to this direction, showing a diminished cell killing of high dose rate and dose per impulse electrons compared to photons. Thus, the influence of very high dose rates, let alone that due to high doses per impulse, is far from being clear, which justifies further research and the need for experimental data.

To date, only a few studies have been performed on actual laser-driven proton-induced biological effects: Kraft et al (2010) described a preliminary experimental set-up for radiobiological studies at the ultra-short 150TW DRACO facility in Dresden , Germany, highlighting the need for further dosimetric and radiobiological studies [15]. Two more recent studies examined the clonogenic survival of the human salivary cancer line HSG to quasimonoenergetic proton beams of 2.5 MeV in 20 ns bunches [96] , and the clonogenic survival of the rodent V79 cell line to laser-accelerated beams up to 10^9 Gy/s in the energy range 0.5 MeV [97]. These studies provided somewhat conflicting results pointing to a higher RBE of laser-driven protons [96] as opposed to the lack of a significant difference in such beams compared to photons [97].

The high-dose rate investigations performed so far have not been addressing the possible issues of complex damage caused by overlapping (in time and space) ionizations from secondary electrons. As biological response is dominated by the degree of damage complexity, estimation of this effect and comparison with more conventional dose rates is paramount for the employment of high-dose rate beams in hadrontherapy. Moreover, the data so far published failed to demonstrate significant differences as a function of the beam dose rate, however most of studies have examined mainly cell survival, thereby overlooking sublethal stress and heritable DNA damage, which are important for long-term consequences in healthy tissue. In this project, we propose to carry out a series of assays on DNA damage and sub-lethal stress responses such as premature cellular senescence, which will provide more thorough information on the cellular response to such peculiarly generated beams. We plan to perform these measurements both with conventional clinical proton beams (using the LNS cyclotron beams at the CATANA facility) and with pulsed laser-driven beams at the TARANIS facility in Belfast and at Flame facility in Frascati. Our aim is to cross-compare the results in order to assess eventually differences in the cell response.

At the irradiation facilities for protons and carbon ions at LNS, a series of experiments was performed with the aim to investigate very radioresistent cell lines. The choice of such a limit case of cellular radiosensitivity was based on the need to find out how far protons and carbon ions could reach in their inactivation [111, 112, 113]. This was particularly important since the large majority of the radiobiological studies were focused on the radiosensitive cell lines. To boost the level of inactivation of the radioresistant cells also combined treatments involving different types of the radiation and anticancer drugs were studied [114, 115].

13.5.2 Objectives

The main objective is to evaluate and differentiate among the effects elicited both by high dose rate and pulsed beams on normal and cancer cells. Primary dermal human fibroblasts, a typical normal cell line, and DU145 prostate cancer cells will be used. The extent of the long-term damage to the healthy tissue is still undetermined in hadrontherapy, while prostate cancer represents one of the types of tumour of choice by charged particle therapy. In particular, we aim at studying the dependence of biologically relevant effects from the beam dose rates and beam pulse frequency by measuring the Relative Biological Effectiveness (RBE) of the tested irradiation regimes by means of the clonogenic cell survival assay, the induction of DNA damage and its repair kinetics by comet assay and immunofluorescence, and the onset of premature cellular senescence, which is useful to investigate as a non-cancer late effect of radiation possibly affecting tissue physiological homeostasis. Moreover we will determine the levels of Reactive Oxygen Species (ROS) responsible for the indirect effects of radiation, being also considered to be important signal molecules for the cell and possibly responsible for the perpetuation of late-occurring effects such as genomic instability. Finally, we will analyze different pathways involved in cellular response to radiation, particularly some cellular processes such as apoptosis, DNA repair and oxidative stress response by analysis of gene expression (measured with Affymetrix GENE chip Human Genome U133 plus platform), with a method based on ”gene enrichment” with "a priopri biological knowledge" (hypergeometric distribution method) [98, 99]. In addition, we propose to implement the experimental set-up ARETUSA developed at LNS-INFN for the single photon counting measurement of the low-level photoinduced Delayed Luminescence (DL). By this approach we were able to discriminate between normal cell and tumoral ones [100] and recently we have correlated the DL signal intensity to apoptosis level induced in leukemia cells [101, 102]. Thus, we shall compare the results of this technique with those obtained from both Comet assay and gene expression analysis, which will in turn help to develop an on-line diagnostic technique that could provide real-time information on the effects of treatments on the cells.

13.5.3 Outline of the experimental plan

A first series of radiobiological experiments will be performed at LNS using conventional proton beams to be compared against very high-dose rate protons. Adequate dosimetry will have to be implemented as discussed earlier. Results will also be compared to those obtained irradiating cells with low-LET radiation used as reference for RBE calculations.

The involved groups have long-standing experience in cell culture techniques and radiobiology. During this phase, a dose rate of about 10 Gy min^{-1} will be assumed as "conventional", since it is comparable to that routinely used at LNS in the proton treatment of ocular cancer, in contrast to a very high dose rate of about 500 Gy min^{-1}. Cells will be grown in standard tissue culture flash at the biological facility of LNS and after irradiation the above-listed endpoints will be investigated (i.e., cell survival, DNA damage and repair, cellular senescence, gene expression and reactive oxygen species levels , apoptosis by photoinduced delayed luminescence). These preliminary tests at LNS will then be followed by irradiations using laser-accelerated protons at various facilities. This will allow us to compare the results obtained with protons conventionally accelerated at very high dose rates with those from beams whose temporal structure will be significantly different, thereby bearing biological consequences. In particular, the second phase (2014 - 2015) foresees to employ proton beams accelerated by existing laser sources (Belfast, FLAME and KOREA). The Table below summarizes the endpoints that will investigated and the information that they will convey.

Table 13.1: Biological endpoints that will be investigated during the experiment.

Endpoint	**Assay**	**Information**
Cell death	Colony formation assay	Radiation-Induced loss of proliferative potential
Functional assay	MTT assay	Metabolic components necessary for cell growth
DNA double-strand breaks	Immunochemical detection of γ-H2AX foci	Induction of DSBs and kinetics of repair
Different DNA damage and repair capability	Comet Assay	Evaluation of DNA fragmentation and/or repair capacity of irradiated cells
Cellular senescence	Beta-galactosidase Assay	Determination of cellular premature senescence induced by radiation
Gene expression measurements	Affymetrix GENE chip Human Genome U133 plus	Determination of genes and pathways involved in response to radiation
Reactive Oxygen Species (ROS) measurements	Fluorescence Microscope Analysis with H_2DFFDA and DHE	Quantification of the level (concentration) of ROS following exposure to radiations

14 Planned experimental sections

14.1 TARANIS Facility at Queen's University (UK)

The **TARANIS** laser is a hybrid $Ti : Sapphire - Nd - glass$ system operating in the chirped pulse amplification mode. This unique laser model can simultaneously deliver two 1053 nm beams in each of the two existing target areas, in different combinations of 700 $fs/1$ ns pulse and with intensities up to 10^{19} W/cm^2 in the short pulse mode and up to 30 J on target in the ns pulse mode. The laser rep rate is 1 shot every 10 minutes [103]. The laser front-end consists of a Ti:Sapphire oscillator, followed by a folded all-reflective stretcher, and by a Ti:Sapphire regenerative amplifier (RA). The oscillator provides a train of transform-limited, 120 fs long pulses at a wavelengh of 1053 nm, with a repetition frequency of 76 MHz. The wavelengh is chosen to match the peak of the Nd:glass amplifiers gain curve in the glass amplification chain, and, although the gain of the Ti:Sapphire crystal is not peaked at 1053 nm, the oscillator delivers an average power of 400 mW. Pulse stretching is achieved within the double-pass stretcher, equipped with diffraction grating and a spherical mirror, arranged in an inverting telescope configuration. The stretcher bandpass is chosen to be about 4 times the oscillator output bandwith and the streching factor is about 10^4, providing at the output 1.2 ns long optically chirped pulses. Pre-amplification of the laser pulse is obtained in the Ti:Sapphire RA, pumped by a Q-switched Nd:YLF laser operating at the wavelengh of 527 nm. Optimization of the Ti:Sapphire RA for amplification at 1053 nm and a double set of Pockels cells located after the RA cavity contribute to limiting and controlling amplified spontaneous emission and pre-pulse activity. Amplification to multi-TW levels is achieved within a three stage Nd:glass amplification chain , optically pumped with flash lamps. As a result of the tailoring (by 3.4 mm diameter serrated aperture, located at the input of the glass amplification chain) and relay-imaging (by spatial filters between the different amplifications stages), the beam conserves a near-uniform top-hand spatial profile through the amplification chain, allowing optimal energy extraction from the glass rods. The two pulses from the glass amplification chain can be separately re-compressed in two double pass grating compressors.

A maximum proton energy of ~ 12 MeV was obtained with 10 μm thick aluminum targets [104]. The typical proton spectrum has been used to perform some preliminary dose evaluation of the beam selected with the first prototype of energy selector. The selecting device is placed 1.5 m far from the target. The collimator has 1mm diameter and the slit size is 1 mm. Two energies values (4 and 8 MeV) are taken in account. Following table reports data on the simulated energy spread and transmission efficiency.

$Energy$ $[MeV]$	$Energy\,Spread$ $(FWHM/E_0)$	$Simulated\,transmission$ $efficiency$	$Expected\,transmission$ $efficiency$
4	3.5%	7.5%	15%
8	5%	2.6%	4%

According the information on the beam, the total number of particles produced per shot is 1.7763×10^9. After energy selection the expected number of particles are reported in the following table.

	$Particle\ per\ shot\ (out)$
4 MeV	228945
8 MeV	70000

Using the above data, preliminary MC simulation with $Geant4$ have been performed in order to evaluate the amount of dose delivered to a water phantom per each shot. Results are reported in the following table.

Number of Particle per Pulse	Incident Energy (MeV)	SD of Incident Energy (keV)	Phantom Length (mm)	Lateral Dimension of Phantom (mm)	Peak Position (μm)	Absorbed Dose (mGy)
70000	8	169.8643	1	4×4	765	5.47873
228945	4	59.45	0.4	4×4	205	21.1206

In order to calculate the dose as a function of the depth, phantom is divided to slices with 0.01 mm length. Depth dose profile related to 8 MeV protons is reported in Figure 14.1.

14.2 GIST Facility (Republic of Korea)

In the **GIST** Laboratory, in Gwangju (Korea), there is a 0.1 Hz, 1.0 PW CPA $Ti:Sapphire$ laser system, the typical pulse duration is 30 fs (FWHM). This laser system is shown to have very low energy fluctuation and an almost homogeneous flattop spatial profile; it consists of a 1 kHz multi-pass amplifier system, a grating stretcher, a preamplifier,

Figure 14.1: Depth dose profile specified by colour for 8MeV proton beam

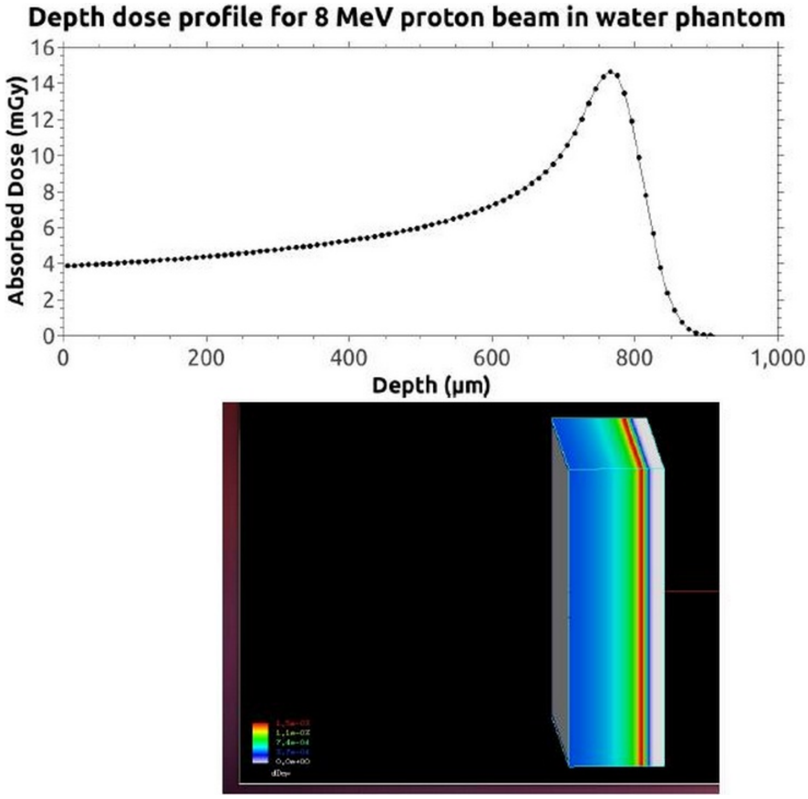

two power amplifiers, a final three-pass booster amplifier, and a grating compressor. A commercial 1 kHz multi-pass amplifier system is used as a front end to provide seed pulses for the amplifiers. Laser pulses from the 1 kHz amplifier system are stretched to about 0.9 ns with a grating. After stretching, the laser pulse is amplified in the preamplifier and the two power amplifiers thus its energy reaches 4.5 J. Before being injected into the final booster amplifier, the amplified laser pulses are upcollimated to a 60 mm diameter optical aperture through an achromatic beam expander. After passing through the expander, the laser pulses are amplified in the final three-pass booster amplifier. An $Nd : glass$ laser system (527 nm laser pulses in 12 beams at a 0.1 Hz repetition rate, each of the 12 beams delivers 8.0 J of energy) is used to pump the final booster amplifier. The measured spatial beam profile is close to a homogeneous flattop and agrees well with the calculated profile. From the laser beam image of the central area occupying 80% of the whole energy, the standard deviation of the intensity level in the central area was calculated. The standard deviation was found to be 13% in the central area. Note that this homogeneous flattop spatial beam profile could be achieved with no image relay method or spatial filter. There is also a good reproducibility shot-to-shot, for example the shot-to-shot fluctuation for 25 successive laser pulses was as low as 0.53% in rms value.

14.3 PALS Facility in Prague (CZ)

The terawatt iodine laser system **ASTERIX IV** is implemented in Prague, at **PALS** Laboratory. It is a single beam iodine photodissociation laser system, based on a Master Oscillator-Power Amplifier (MOPA) configuration. It supplies up to 1 kJ of energy at the fundamental wavelength 1.315 nm, in pulses of 400 ps duration.
The lasing medium is composed of a mixture of perfluoralkyliodide C_3F_7I and Ar acting as a buffer gas that reduces the small-signal amplification. The lasing action occurs on the magnetic dipole type transition between the two fine structure levels of ground state doublet of the iodine atom

$$I(5\,^2P_{1/2}) \longmapsto I(5\,^2P_{3/2}) + h\nu(1.315mm)$$

produced by a photodissociation of C_3F_7I by UV light in the region 240-300 nm, generated by Xe flash-lamps:

$$C_3F_7I + h\nu(240-320nm) \longmapsto C_3F_7I + I(5\,^2P_{1/2})$$

The primary pulse is generated in an opto-acoustical mode-locked oscillator equipped with a high-extinction ratio pulse selection system (contrast ratio 10^9). This pulse is seeded into a chain of one preamplifier and five power amplifiers separated by spatial filters which remove the high spatial components from the angular beam spectrum and simultaneously act as image relay pairs ensuring optimum coupling between adjacent amplifiers through increasingly large diameter sections. The beam at the output of the last amplifier is 29 cm in diameter. According to the need of a given experiment it may be frequency doubled to 658 nm or tripled to 438 nm, using the $DKDP$ (deuterated potassium dihydrogen phosphate) crystals, prior to the final focusing down into the target chamber. At the present arrangement, the conversion efficiency of up to 60% and 30% is expected at 3ω at 2ω, respectively. The characteristic feature of both the fundamental and frequency up-converted output beam is a high spatial uniformity, typically within 66% of the mean value. The laser is capable to fire a full-energy shot each 20 minutes, delivering on the target in the vacuum interaction chamber the focused power density up to 3×10^{16} W/cm^2, the focal spot on target is 50-70 μm and the spatial uniformity is very high (±6% of the average value).

14.4 FLAME Facility at LNF-INFN (I)

The **FLAME** laser system is a CPA laser, with $Ti:Sapphire$ as active medium. It supplies up to 250 TW of power at the fundamental wavelength 800 nm, in pulses of 25 fs duration, with a repetition rate of 10 Hz. FLAME project, as other new generation laser system, looks for an improvement of the beam temporal profile (ASE contrast of 10^{-9}), shot-to-shot energy stability (0.77% rms of the energy) and the high beam spatial quality. It consists of an oscillator, a booster (the main innovative part for the improvement of the temporal contrast), a grating stretcher, a regenerative amplifier, two multi-pass amplifier and a final power amplifier.

LILIA project have been established in order to study and characterize the beam produced in FLAME facilty. In phase **1** laser intensities up to $10^{20} W/cm^2$ are expected and proton with energy up to 6 MeV will be produced. A bunch of 10^{10} protons compatible with those characteristics have been simulated with a PIC code. The bunch have been used to perform a simulation on the energy selector and results are reported in the following table.

	$Particle\ per\ shot\ (out)$
4 MeV	228945

In phase two the highest laser intensity will be reached using adaptive optics. The maximum proton energy will be about 30MeV using thin metal targets. A bunch of 10^{10} protons compatible with those characteristics have been simulated with a PIC code. The bunch have been used to perform a simulation on the energy selector and results are reported in the following table.

	$Particle\ per\ shot\ (out)$
4 MeV	142500
8 MeV	104000

The high laser rep rate could allow a great increasing in the number of protons selected. Using the above data, preliminary MC simulation with Geant4 have been performed in order to evaluate the amount of dose delivered to a water phantom per each shot. Results reported in the following table are related to the first phase of the project.

Number of Particle per Pulse	Incident Energy (MeV)	SD of Incident Energy (keV)	Phantom Length (mm)	Lateral Dimension of Phantom (mm)	Peak Position (μm)	Absorbed Dose (mGy)	Total Energy Deposition (MeV)
217500	4	59.45	0.4	4×4	205	20.0646	801494.772

Results for high energy particles available in the next phase are reported in the table below.

Number of Particle per Pulse	Incident Energy (MeV)	SD of Incident Energy (keV)	Phantom Length (mm)	Lateral Dimension of Phantom (mm)	Peak Position (μm)	Absorbed Dose (mGy)	Total Energy Deposition (MeV)
104000	8	169.8643	1	4×4	765	8.14129	813022.702
142500	4	59.45	0.4	4×4	205	13.14591	525120.57

15 Financial plan

15.1 WP1

INVENTORY	Tot	2013	2014	2015
ICCD Andor Istar for time resolved imaging equipped with a -03 photocathode model Gen2 MGS<2ns (WP-1.3)	45 kE	45 kE		
Monochromator (WP-1.3)	15 kE		15 kE	
Ultrafast programable 6 channels gate generator (WP-1.3)	7 kE	7 kE		
CDD ANDOR IKON-M (40 to 95% QE efficiency in the region 60 eV-1000 eV) (WP-1.4: X-Ray spectroscopy and imaging)	27 kE	27 kE		
X-Ray grating in the region 1-5 nm (WP-1.4: X-Ray spectroscopy and imaging)	17 kE	17 kE		
X-Ray grating in the region 5-20 nm (WP-1.4: X-Ray spectroscopy and imaging)	12 kE		12 kE	
N.1 Pepper pot emittance meter (WP-1.2)	5 kE	5 kE		
Fast digitiser DT5742, 16 channels (WP-1.2)	10 kE		10 kE	
Vacuum system for the magnetic spectrometer (WP-1.2)	6 kE	6 kE		
TOTAL	144 kE	107 kE	37 kE	0 kE

APPARATUS	Tot	2013	2014	2015
Thomson Spectrometer upgrade (WP-1.2: collimation system, optimisation of the detector FOV, alignment system)	10 kE	10 kE		
Fulfillment 32 IC magnetic spectrometer (WP-1.3)	6 kE		6 kE	
Ion collector (n.1)/year and Ion collector rings (n.1)/year with different absorbers (WP-1.2)	12 kE	4 kE	4 kE	4 kE
TOTAL	28 kE	14 kE	10 kE	4 kE

CONSUMABLE	Tot	2013	2014	2015
Chemical for nano-structures production (WP-1.1)	20 kE	12 kE	4kE	4 kE
SiC detector for TOF techniques (n.1)/year with different absorbers (WP-1.2)	6 kE	2 kE	2 kE	2 kE
Monocristal diamond detectors(n.1)/year (WP-1.2)	6 kE	2 kE	2 kE	2 kE
Optics and filter (WP-1.3)	7 kE	4 kE	2 kE	1 kE
Material for mechanic devices (WP-1.2)	6 kE	2 kE	2 kE	2 kE
Scintillator for alternative detector for the TP (WP-1.2)	1 kE	1 kE		
Cables and various material to support the measure at PALS and at LNS with the conventional cyclotron beams (All WPs)	5 kE	2 kE	2 kE	1 kE
TOTAL	51 kE	25 kE	14 kE	12 kE

15.2 WP2

APPARATUS	Tot	2013	2014	2015
Magnets (PM and iron yokes construction) and assembly (WP-2)	12 kE	12 kE		
Vacuum Chamber (WP-2)	11 kE	11 kE		
Selection slit system fully motorized and remote controlled (WP-2)	5 kE	5 kE		
Magnet moving system (amagnetic roller guide and motors X-Y direction) remote controlled (WP-2)	8 kE		8 kE	
Controll system (WP-2)	3 kE		3 kE	
Support Aluminium made (WP-2)	1 kE		1 kE	
Beam collimator system (upstream and downstream) (WP-2)	4 kE		4 kE	
Laser alignment system (WP-2)	4 kE		4 kE	
TOTAL	48 kE	28 kE	20 kE	0 kE

15.3 WP3

INVENTORY	Tot	2013	2014	2015
In-air faraday cup (WP-3.3: current measurements)	4 kE		4 kE	
N.2 plastic scintillators + N.2 photomultipliers (WP-3.2: innovative in transmission system for the on-line beam monitoring)	6 kE	3 kE	3 kE	
N.2 pocket MCA system (WP-3.2)	9 kE	4.5 kE	4.5 kE	
N.2 HV Supply 2000 V Low Ripple (WP-3.2)	8 kE	4 kE	4 kE	
N.2 RS232 converters (WP-3.2)	1 kE	0.5 kE	0.5 kE	
N.1 PC for data acquisition (WP-3.2)	1 kE	1 kE		
N.2 PC for Monte Carlo calculation (WP-2.2 and WP-3.1)	2 kE	1 kE	1 kE	
TOTAL	31 kE	14 kE	17 kE	0 kE

APPARATUS	Tot	2013	2014	2015
Mechanical system for dosimetry and radiobiology samples positioning (WP-3.3 and WP-3.4)	15 kE	15 kE		
Secondary emission monitor for proton beam fluence measures (WP-3.3)	3 kE		3 kE	
TOTAL	18 kE	15 kE	3 kE	0 kE

CONSUMABLE	Tot	2013	2014	2015
Gafchromic detectors (WP3.3)	6 kE	2 kE	2 kE	2 kE
CR39 detectors (WP-3.3, WP-1.2)	5 kE	2 kE	2 kE	1 kE
Cables for the on-line monitoring (WP-3.2: innovative in transmission system for the on-line beam monitoring)	2 kE	2 kE		
N.2 lead battery deep-cycle + DC-AC converter (WP-3.2)	1 kE	0.5 kE	0.5 kE	
Scattering foils (WP-3.2)	1 kE	1 kE		
Material for radiobiological irradiations with conventional beams and at laser facilities (WP-3.4)	30 kE	10 kE	10 kE	10 kE
TOTAL	45 kE	17.5 kE	14.5 kE	13 kE

15.4 National and International Travel

NATIONAL TRAVEL	Tot	2013	2014	2015
Domestic travels for collaboration workshop and runs at LNS (All WPs)	36 kE	16 kE	10 kE	10 kE
Test at the FLAME facility of the Thomson spectrometer (3 researcher for 3 weeks at LNF, s.j.)(All WPs)	15 kE	5 kE	5 kE	5 kE
TOTAL	51 kE	21 kE	15 kE	15 kE

INTERNATIONAL TRAVEL	Tot	2013	2014	2015
PALS (Prague-Cz) run already approved in January-March period (All WPs)	34 kE	18 kE	16 kE	
TARANIS (Belfast-UK) run (late 2013 in s.j.) for Energy Selector Testing at hight energy (All WPs) GIST (Gwangju-Kr) run (2015 s.j.) for Energy Selector Testing at high energy (All WPs)	39.5 kE 15 kE	14.5 kE	25 kE	 15 kE
TOTAL	88.5 kE	32.5 kE	41 kE	15 kE

15.5 Transport

TRANSPORT	Tot	2013	2014	2015
Transport to laser international laboratories (all WPs)	33 kE	5 kE(PALS) 5 kE (TARANIS,s.j.)	5 kE (PALS) 5 kE (TARANIS, s.j.)	8 kE (GIST, s.j.) 5 kE (FLAME,s.j.)

16 MILESTONES, DERIVABLE AND TEMPORAL PLAN

WP	Milestones 2013	Deliverable 2013
All WPs	Periodic report in slides and/or text format of each WPs	Report 1 - Apr. 2013 Report 2 - Ago. 2013 Report 3 - Dec. 2013 (final report)
WP-1: Target, PIC simulations, plasma and laser-driven beams diagnostic (WP-1.1, WP-1.2, WP-1.3, WP-1.4)	**M-1.1.a:** Realisation and test of nanostructured and porouses targets up to 1 micron thickness **M-1.2.a:** Test and data analysis of IC, ICR, SiC and Diamonds using TOF approach at PALS laboratory (I=10^{16} W/cm^2) - Dec. 2013 **M-1.2.b:** Upgrading of the Thomson spectrometer - Dec. 2013 **M-1.3.a:** Test of time resolved imaging with ICCD and optics at LNS and/or PALS- April 2013 **M-1.4.a:** ED-XRS measurements and 2D X-ray imaging in different energy domains of brilliant plasma source - April 2013 **M-1.4.b:** Design and development of the new High Resolution X-Ray Spectrometer - Sept. 2013 **M-1.4.c:** Feasibility studies of Time-resolved X-ray imaging and spectroscopy by using ancillary MCP detectors coupled to X-ray diagnostic tools - May 2013	**D-1.1.a1:** Realization and preliminary test of realized targets based on nanostructured and porouses materials - Jun. 2013 **D-1.1.a2:** Realization of nanostructured targets with thicknesses of the order of 1 micron - Dec 2013 **D-1.2.a1:** Experimental tests of IC, ICR, SiC and Diamonds using TOF approach at PALS laboratory (I=10^{16} W/cm^2) - April. 2013 **D-1.2.a2:** Data analysis aimed to enhance the detector efficiency to detect selectively protons with respect to other ion and photon species. The new detector will be employed for the planned experiments at the TARANIS (Belfast, UK) and/or at the FLAME(if available) facility - Dec 2013 **D-1.2.b:** Complete upgrade of the Thomson spectrometer for final test at the TARANIS (Belfast, UK) and/or at the FLAME facility (if available)- Dec 2013 **D-1.3.a:** Report about measurements of the two dimensions time resolved imaging of a plasma plume **D-1.4.a:** Integrated measurements with X-ray based techniques suited for the space-resolved imaging and spectroscopy of EUV and X radiation (from to 60 eV up to 100 keV) emitted by Laser-generated hot-plasma - April 2013 **D-1.4.c:** Report on time-resolved analysis by using ancillary MCP detectors coupled with X-ray pinhole and High Resolution X-ray Spectrometer - Dec. 2013
WP-2. Energy selection system and beam transport (WP-2.1, WP-2.2, WP-2.3)	**M-2.1.a:** Study of the beam optics: Solenoid and quadrupole focusing system **M-2.2.a:** Monte Carlo Simulation of the ESS **M-2.3.a:** Design, Construction and Assembly of the Energy Selector System (ESS) **M-2.3.b:** Preliminary calibration of the ESS (TANDEM at LNS or CN at LNL)	**D-2.1.a:** Preliminary Result Report (April 2013); Status of Beam Optic Study - November 2013 **D-2.2.a:** Preliminary Result Report - October 2013 **D-2.3.a:** Report on the Design Study of the ESS -June 2013 **D-2.3.b:** Status Report on ESS Calibration measurements - November 2013
WP-3. Hadrontherapy transport, dosimetry and radiobiology (WP-3.1, WP-3.2, WP-3.3, W-P3.4)	**M-3.1.a:** Monte Carlo simulations for the evaluation of dose distribution in different experimental configurations **M-3.2.a:** Full assembling of the first ELImon prototype, on-line monitor detector **M-3.2.b:** In-beam test of the ELImon prototype (PALS and Belfast facilities) **M-3.3.a:** Study and design of a dosimetric system for the irradiation of dosimetry and biological samples (Dec. 2013) **M-3.3.b:** Design and development of a dedicated Faraday Cup for absolute dose measurements **M-3.3.c:** GafChromic measurements **M-3.4.a:** Radiobiological measurements at very high dose rates for conventionally accelerated protons	**D-3.1.a1:** Simulation of the PALS (Prague) experimental setups for gafchromic dose delivered predictions (June 2013) **D-3.1.a2:** Simulation of the TARANIS (Belfast) experimental setups for gafchromic dose delivered predictions (Dec. 2013) **D-3.2.a:** Design report of ELImon (mid 2013) **D-3.2.b:** Performance validation of the first ELImon prototype (mid-end 2013) **D-3.3.a1:** Design of the dosimetric system (June 2013) **D-3.3.a2:** Realisation of dosimetric system (Dec. 2013) **D-3.3.b1:** Design of the FC (April 2013) **D-3.3.b2:** First prototype of the FC (June 2013) **D-3.3.b3:** Test of the FC under conventional CS beams (Dec 2013) **D-3.3.c:** Calibrations and characterization at LNS-INFN wit 62 MeV proton beams **D-3.4.a:** Optimization of the irradiation protocol (dose range, dose rates, time schedule for data collection)

WP	Milestones 2014	Deliverable 2014
All WPs	Periodic report in slides and/or text format of each WPs. Coordinator of each WP is responsible for each report. Submission of a beam request proposal at RAL Lab. (UK) (s.j.)	Report 1 - Feb. 2014 (in preparation of the final report relative on 2013) Report 2 - Ago. 2014 Report 3 - Dec. 2014 (final report)
WP-1: Target, PIC simulations, plasma and laser-driven beams diagnostic (WP-1.1, WP-1.2, WP-1.3, WP-1.4)	**M-1.1.a:** Use of nanostructured targets to be irradiated at the TARANIS (Belfast, UK) Laboratory. Use of special IC, ICR, SiC and Diamonds to detect protons above 10 MeV with high sensitivity and high energy resolution - Dec 2014 **M-1.2.a:** Analysis of data obtained with IC, ICR, SiC and Diamonds at Belfast Lab (I = 10^{18} W/cm^2) in order to have information on the angular distribution in forward and in backward direction. Evaluation of the proton energy distribution and comparison with the TP measurements **M-1.3.a:** Use of a VIS and UV ICCD for plasma diagnostic at Belfast lab **M-1.4.a:** Use of X-ray based techniques for plasma diagnostic at Belfast lab- Dec. 2014	**D-1.4.a:** Analytical Results obtained by ED-XRS, HR-XRS and XRI measurements at Belfast lab, focused to determine density, temperature, state of charges and energy of electrons and ions in plasma produced by the laser interaction - Dec. 2014
WP-2. Energy selection system and beam transport (WP-2.1, WP-2.2, WP-2.3)	**M-2.1.a:** Feasibility Study of the Solenoid Magnet **M-2.2.a:** Validation of the MC simulation about the ESS with experimental data **M-2.3.a:** Test and Calibration of the ESS at the TARANIS (Belfast, UK)- Feb. 2014	**D-2.1.a:** Preliminary Report on the feasibility Study of Solenoid Magnet and Power Supply- April 2014 Final Report - Nov 2014 **D-2.2.a:** Status Report - May 2014 **D-2.3.a:** Status Report on ESS Commission - Jun 2014
WP-3. Hadrontherapy transport, dosimetry and radiobiology (WP-3.1, WP-3.2, WP-3.3, W-P3.4)	**M-3.1.a:** Monte Carlo simulation of the different dosimetry detectors **M-3.2.a:** Design of the ELImon mechanical set-up (target frame and detector holder) **M-3.2.b:** Assembly of two detector modules **M-3.3.a:** Functioning tests of the dosimetric device and first irradiation at the TARANIS facility (Belfast, Uk) - Dec. 2014 **M-3.3.b:** Test of the FC prototype at the TARANIS facility (Belfast, UK), integration of the FC in the complete dosimetric system and cross-comparison with transmission ionization chambers - Dec. 2014 **M-3.3.c:** GafChromic dosimetry **M-3.4.a:** Comparison of cellular response between laser-driven beams (TARANIS facility, Belfast, UK) and very high dose rate beams accelerated conventionally (INFN-LNS, Catania)- Dec. 2014	**D-3.1.a1:** Simulation of Gafchromic, CR39 and Faraday cup response- June 2014 **D-3.1.a2:** Simulation of the final configuration of the integrated dosimetry system (Dec 2014) **D-3.2.a1:** Design report of the final mechanical set-up (mid 2014) **D-3.2.a2:** Test report of the ELImon set-up simulating the final beam-line arrangement (sept-oct 2014) **D-3.3.a1:** Functioning tests of the irradiation device at LNS under conventional beams - Jun 2014 **D-3.3.a2:** First irradiation at the TARANIS facility (Belfast, Uk) - Dec. 2014 **D-3.3.b1:** Report on the developed FC (Feb. 2014) **D-3.3.b2:** FC and ionization chamber test with the laser-driven protons of the TARANIS facility (Belfast, UK) - Jun. 2014 **D-3.3.b3:** Design of the FC integrated in the dosimetric system and complete integration of the FC in the final dosimetric system -Dec. 2014 **D-3.4.a:** Discrimination of sensitivity and variation in cellular response between the various assays (e.g. cell survival vs. DNA damage or ROS production)

WP	**Milestones 2015**	**Deliverable 2015**
All WPs	Periodic report in slides and/or text format of each WPs	Report 1 - Feb. 2015 (in preparation of the final report relative on 2014) Report 2 - Ago. 2015 Report 3 - Dec. 2015 (final report)
WP-1: Target, PIC simulations, plasma and laser-driven beams diagnostic (WP-1.1, WP-1.2, WP-1.3, WP-1.4)	**M-1.1.a:** Use of target realized at ultra intense laser lab for TNSA irradiation. The target geometry and structure will be devoted to promote resonant absorption effects, maximum proton energy and narrow energy spread **M-1.2.a:** Measurements with IC, ICR, SiC an Diamonds at Ultraintense laser labs (>10^{19} W/cm^2). Such detector will be improved to be used in TOF approach measuring the proton and other ion contributions **M-1.3.a:** Use of a VIS and UV ICCD for plasma diagnostic at ultra intense laser lab **M-1.4.a:** Use of X-ray based techniques for plasma diagnostic at ultra intense laser lab (early 2015, to be established by the collaboration)	**D-1.4.a:** Definition of the analytical protocol based on the integration of X-rays diagnostic tools for the comprehensive characterization of plasma induced by laser in different target material - Dec. 2015
WP-2. Energy selection system and beam transport (WP-2.1, WP-2.2, WP-2.3)	**M-2.1.a:** Final Design of the beam Trasport line for ELIMED **M-2.2.a:** Monte Carlo simulations for radio-protection studies related to the ESS	**D-2.1.a:** Report on the Beam Transport line for ELIMED - Jun. 2015 **D-2.2.a:** Status Report- Dec. 2014
WP-3. Hadrontherapy transport, dosimetry and radiobiology (WP-3.1, WP-3.2, WP-3.3, W-P3.4)	**M-3.1.a:** Monte Carlo simulation of the in air transport beam line for the ELIMED facility and radioprotection assessments **M-3.2.a:** assembling and commissioning the final ELImon set-up at the test facilities **M-3.3.a:** Irradiation tests at FLAME facility (if available) and/or at the GIST facility (Gwangju, Republic of Korea) - Dec. 2015 **M-3.3.b:** FC and Ionization Chamber measurements with the FLAME (Frascati, IT) beams (if available) and/or and GIST beams (Gwangju, Republic of Korea) - Dec 2015 **M-3.4.a:** Determination of conclusive RBE values of high-energy laser-driven protons for all major endpoints	**D-3.1.a:** Simulation of passive/active elements for the beam shaping and dose delivery at the measurement point; preliminary evaluation of the radioactive activation for shielding design **D-3.2.a1:** Final report of ELImon: performances and specifications **D-3.2.a2:** ELImon user manual **D-3.3.a1:** Report on the first tests with the irradiation system coupled with the energy selector - Jun. 2015 **D-3.3.a2:** Verification of the possibility to move at FLAME or GIST the irradiation system (IS) with the energy selector - Apr. 2015 **D-3.3.a3:** The IS with the Energy Selector System (ESS) should be installed at FLAME or GIST - Oct. 2015 **D-3.3.b1:** Report on the FC and Ionization Chamber activity - Mar. 2015 **D-3.3.b2:** Final dosimetric measurements at the available facilities - Dec. 2015 **D-3.4.a:** Accumulation of radiobiological data at very high dose rates and ultra-short dose pulses

REFERENCES

[1] INFN (2012), *Piano Triennale dell'INFN 2012-14*

[2] L. Laska et al., Experimental studies of generation of 100 MeV Au-ions from the laser-produced plasma
Laser and Particle Beams 27 (2009) 137Ð147.

[3] J. Krasa et al., Generation of high currents of carbon ions with the use of sub-nanosecond near-infrared laser pulses
Rev. Sci. Instr. 81 (2010) 02a504.

[4] D. Margarone et al., New methods for high current fast ion beam production by laser-driven acceleration
Rev. Sci. Instr. 81 (2010) 02a506.

[5] D. Margarone, et al., High current, high energy proton beams accelerated by a sub-nanosecond laser
Nucl. Instr. and Meth. A, 653 (2011) 159

[6] S.C. Wilks et al. Energetic proton generation in ultra-intense laser-solid interactions
Phys. Plasmas 8 542, 2001.

[7] E. L. Clark et al., Energetic Heavy-Ion and Proton Generation from Ultraintense Laser-Plasma Interactions with Solids
Phys. Rev. Lett. 85 (2000) 1654.

[8] L. Torrisi et al., Tantalum ions production by 1064 nm pulsed laser irradiation
J. Appl. Phys. 91(5), 4685-4692, 2002

[9] P. McKenna et al., High-intensity laser-driven proton acceleration: influence of pulse contrast
Phil. Trans. R. Soc. A (2006) 364, 711.

[10] E. L. Clark et al. Energetic heavy-ion and proton generation from ultraintense laser-plasma interactions with solids
Phys. Rev. Lett. 21(85-n.8), 1654, 2000.

[11] L. Torrisi, G. Foti, L. Giuffrida, D. Puglisi, J. Wolowski, J. Badziak, P. Parys, M. Rosinski, D. Margarone, J. Krasa, A. Velyhan and J. Ullschmied, Single crystal silicon carbide detector of emitted ions and soft x-rays from power laser- generated plasmas
J. Appl. Phys. 105, 123304 (2009).

[12] L. Torrisi, D. Margarone, L. Laska, M. Marinelli, E. Milani, G. Verona-Rinati, S. Cavallaro, L. Ryc, J. Krasa, K. Rohlena and J. Ullschmied, Monocrystalline diamond

detector for ionizing radiation emitted by high temperature laser-generated plasma *J. of Appl. Physics* 103, 083106, 1-6, 2008.

[13] D. Margarone, J. Krasa, L. Laska, A. Velyhan, T. Mocek, J. Prokupek, E. Krousky, M. Pfeifer, S. Gammino, L. Torrisi, J. Ullschmied and B. Rus, Measurements of the highest acceleration gradient for ions produced with a long laser Pulse *Review of Scientific Instruments* 81, 02A506, 2010.

[14] M. J. Rhee, Compact Thomson spectrometer *Rev. Sci. Instrum.* 55 (8), August 1984.

[15] R. F. Schneider, C. M. Luo, M. J. Rhee, Resolution of the Thomson spectrometer *J. Appl. Phys.* 57 (1), 1 January 1985.

[16] D. Jung, R. Horlein, D. Keifer, S. Letzring, D. C. Gautier, U. Schramm, C. Hubsch, R. Ohm, B. J. Albright, J. C. Fernandez, D. Habs, B. M. Hegelich, Development of a high resolution and high dispersion Thomson parabola *Review of Scientific Instruments* 82(1):013306, 2011.

[17] K. Harres, M. Schollmeier, E. Brambrik, P. Audebert, A. Blaevi, K. Flippo, D. C. Gautier, M. Geibel, B. M. Hegelich, F. Nurnberg, J. Schreiber, H. Wahl, M. Roth Development and calibration of a Thomson parabola with microchannel plate for the detection of a laser-accelerated MeV ions *Rev. Sci. Instrum.* 79, 093306 (2008).

[18] G. A. P. Cirrone, G. Cuttone, M. Maggiore, L. Torrisi, F. Tudisco, Diagnostic for the radiotherapy use of laser accelerated proton beams *Radiation Effects and Defects in Solids* Vol 00, No. 00, January 2008,1-7.

[19] M. Maggiore, S. Cavallaro, G. A. P. Cirrone, G. Cuttone, L. Giuffrida, F. Romano, L. Torrisi, Design and realisation of a Thosom Spectrometer for Laser Plasma Facilities *Nejaka Hlavicka* 123(2020), 123-456.

[20] K. Jungwirth et al, The Prague ASTERIX Laser System *Physics of Plasmas* Volume 8, number 5, May 2001.

[21] D. Jung, R. Horlein, D. Keifer, S. Letzring, D. C. Gautier, U. Schramm, C. Hubsch, R. Ohm, B. J. Albright, J. C. Fernandez, D. Habs, B. M. Hegelich, Development of a high resolution and high dispersion Thomson parabola *Review of Scientific Instruments* 82(1):013306, 2011.

[22] A. Pappalardo, L. Cosentino, and P. Finocchiaro, An imaging technique for detection and absolute calibration of scintillation light *Rev. Sci. Instrum.* 81, 033308 (2010); doi: 10.1063/1.3360931

[23] J. S. Green, M. Borghesi, C. M. Brenner, D. C. Carroll, N. P. Dover, P. S. Foster, P. Gallegos, S. Green, D. Kirby, K.J. Kirkby, P. McKenna, M. J. Merchant, Z. Najmudin, C. A. J. Palmer, D. Parker, R. Prasad, K.E. Quinn, P. P. Rajeev, M. P. Read, L. Romagnani, J. Schreiber, M. J. V. Streeter, O. Tresca, M. Zepf and D. Neely, Scintillator-based ion beams profiler for diagnostic laser-accelerater ion beams
Laser Acceleration of Electrons, Protons, and Ions; and Medical Applications of Laser-Generated Secondary Sources of Radiation and Particles. Edited by Ledingham, Kenneth W. D.; Leemans, Wim P.; Esarey, Eric; Hooker, Simon M.; Spohr, Klaus; McKenna, Paul. Proceedings of the SPIE, Volume 8079, pp. 807919-807919-8 (2011)

[24] D. B. Geohegan, Diagnostics and Characteristics of Laser Produced Plasma in Pulsed Laser Deposition of Thin films
edited by D. B. Chrisey and G. K. Hubler (John Wiley Sons, New York, 1994).

[25] A. Misra, A. Mitra, and R. K. Thareja,
Applied Physics Letters 74, 929 (1999).

[26] Siegel J, Epurescu G, Perea A, Gordillo-V'azquez F J, Gonzalo J and Afonso
C N 2004 Opt. Lett. 29 2228

[27] N. Gambino, P. Hayden,D. Mascali, J. Costello, C. Fallon, P. Hough, P. Yeates, A. Anzalone, F. Musumeci, S. Tudisco, Dynamics of colliding aluminium plasmas produced by laser ablation
Applied Surface Science (2012).

[28] D. Giulietti et al., X-ray emission from laser produced plasmas
La Rivista del Nuovo Cimento, 21, (1998), pp. 1-101.

[29] I. Mantouvalou et al., Study of extreme ultraviolet and soft x-ray emission of metal targets produced by laser-plasma-interaction
Rev. Sci. Instrum. 82, (2011), art. N. 066103

[30] H.J. Kunze, Introduction to Plasma Spectroscopy, in Spinger Series on Atomic
Optical and Plasma Physics, Spinger, London, 2009, ISBN978-3-642-02232-6.

[31] Castro et al., Comparison between off-resonance and electron Bernstein waves heating regime in a microwave discharge ion source
Review of Scientific Instruments , 82, 2012, art.n. 02B501.

[32] Celona et al. Technical issues related to the design of third generation ECR ion sources
Radiation effects and defects in solids 160, 2005, 457-465.

[33] Mascali et al., Preliminary studies on the X-ray emission from an innovative plasma-trap based on the Bernstein waves heating mechanism, oral presentations at the ÒEuropean Conference on X-ray Spectrometry
EXRS 2012 18-22 June 2012, Vienna

[34] H. Daido, *REP. PROG. PHYS.* 75 (2012) 056401

[35] I. Hofmann et al. *PHYS.REV. ST AB* 14, 031304(2011)

[36] K. Harres et al. *PHYS. of PLA.* 17, 023107 (2010).

[37] M. Schollmeier et al.*PHYS. REV. LET.* 101, 055004 (2008)

[38] A. Yogo et al *NUCL. INST. METH.* A 653 (2011).

[39] M.Nishiuchi et al. *PHYS. REV. SP-AB* 13,071304 (2012).

[40] S. Agostinelli et al., Geant4 - a simulation toolkit
Nucl. Instr. and Meth. in Phys. Res. A, 506, 250, 2003.

[41] J. Allison et al., Geant4 developments and applications
IEEE Trans. Nucl. Sci. 53(1), Part 2, 270, 2006

[42] J. Allison, Facilities and methods: Geant4- a simulation toolkit
Nuclear Physics News Vol. 17, 2 , 20-24, 2007

[43] Cirrone G.A.P. et al.
IEEE Trans. Nucl. Sci. 52 (2005) 262.

[44] G.A.P. Cirrone et al., Hadrontherapy: a Geant4-Based Tool for Proton/Ion-Therapy Studies
Progress in NUCLEAR SCIENCE and TECHNOLOGY Vol. 2, pp.207-212 (2011)

[45] Romano F. et al., Applications of Monte Carlo methods to special radiotherapeutic techniques
IL NUOVO CIMENTO C vol. 034 (01), pp. 167-173 (2011). ISSN: 2037-4909

[46] Cuttone G et al., CATANA protontherapy facility: The state of art of clinical and dosimetric experience
THE EUROPEAN PHYSICAL JOURNAL PLUS vol. 126, 65 (2011), ISSN: 2190-5444, doi: 10.1140/epjp/i2011-11065-1

[47] *Bergoz Instrumentation* www.bergoz.com

[48] A. Di Pietro et al.
PRL 105(2010)022701

[49] Richter et al., A dosimetric system for quantitative cell irradiation experiments with laser-accelerated protons
2011 *Phys. Med. Biol.* 56 1529

[50] Daniel Kirby et al., LET dependence of GafChromic films and an ion chamber in low-energy proton dosimetry
2010 *Phys. Med. Biol.* 55 417,

[51] F Fiorini et al. Dosimetry and spectral analysis of a radiobiological experiment using laser-driven proton beams

[52] 2011 *Phys. Med. Biol.* 56 6969.

[53] D. Kirby et al., Radiochromic film spectroscopy of laser-accelerated proton beams using the FLUKA code and dosimetry traceable to primary standards
Laser and Particle Beams June 2011 29 : pp 231-239.

[54] S.D. Kraft et al., Dose-dependent biological damage of tumor cells by laser-accelerated proton beams
New Journal of Physics 12 (2010) 085003

[55] D.S. Hey et al. Use of GafChromic film to diagnose laser generated proton beams
Rev. Sci. Instrum. 79, 053501 (2008)

[56] F. Numberg et al., Radiochromic film imaging spectroscopy of laser-accelerated proton beams
Rev. Sci. Instrum. 80, 033301 (2009)

[57] G.F.Dempsay, Validation of a precision radiochromic film dosimetry system for quantitative two-dimensional imaging of acute exposure dose distributions
Med Phys. 2000 Oct;27(10):2462-75

[58] S.T. Chiu-Tsao, Dose response characteristics of new models of GAFCHROMIC films: Dependence on densitometer light source and radiation energy
Med Phys. 2004 Sep;31(9):2501-8.

[59] O.A. Zeidan, Characterization and use of EBT radiochromic Þlm for IMRT dose veriÞcation
Med Phys. 2006 Nov;33(11):4064-72.

[60] A. Piermattei, Radiochromic film dosimetry of a low energy proton beam
Med Phys. 2000 Jul;27(7):1655-60.

[61] G. Cuttone et al., First Dosimetry Intercomparison Results for the CATANA Project
Physica Medica Vol. XV, No. 3, July-September 1999, 121-130.

[62] G.A.P. Cirrone et al. A 62-MeV Proton Beam for the Treatment of Ocular Melanoma at Laboratori Nazionali del Sud-INFN
IEEE TRANSACTIONS ON NUCLEAR SCIENCE VOL. 51, NO. 3, JUNE 2004.

[63] G. Cuttone et al., CATANA protontherapy facility: The state of art of clinical and dosimetric experience
THE EUROPEAN PHYSICAL JOURNAL PLUS, vol. 126, 65 (2011).

[64] L. Raffaele et al., Dosimetry of clinical proton beams
Rivista Medica, Vol.14, N.1, 2008

[65] M. Martisõkova et al., Dosimetric properties of Gafchromic EBT films in monoenergetic medical ion beams
Phys. Med. Biol. 55 (2010) 3741Ð3751.

[66] L. Zhao et al., Gafchromic EBT film dosimetry in proton beams
Phys. Med. Biol. 55 (2010) N291ÐN301.

[67] S.V. Peterson et al., Experimental validation of a Monte Carlo proton therapy nozzle model incorporating magnetically steered protons
Phys. Med. Biol. 54 (2009) 3217Ð3229.

[68] D. Kirby et al., LET dependence of GafChromic films and an ion chamber in low-energy proton dosimeter
Phys. Med. Biol. 55 (2010) 417Ð433.

[69] L. Karsch, Dose rate dependence for different dosimeters and detectors: TLD, OSL, EBT films, and diamond detectors
Med. Phys. 39, 2447 (2012).

[70] S. Cecchini et al., *Il Nuovo Cimento* 109 A (1996) 1119.

[71] Mukhtar A. Rana , I.E. Qureshi, Studies of CR-39 etch rates
NIM B 198 (2002) 129Ð134.

[72] D.Hermsdorf, Measurement and comparative evaluation of the sensitive V for protons and hydrogen isotopes registration in PADC detectors of type CR-39
Radiation Measurement 44 (2009) 806-812.

[73] A. Szydlowski et al., Application of solid state nuclear track detectors of the CR-39/PM-355 type for measurements of energetic protons emitted from plasma produced by an ultra-intense laser
Radiastion measurements 44(2009) 881-884.

[74] S. Kimura, A. Anzalone, and A. Bonasera, Comment on ”Observation of neutronless fusion reactions in picosecond laser plasmas”
Phys. Rev. E 79, 038401 (2009).

[75] http://rsb.info.nih.gov/ij/, Wayne Rasband (wayne@codon.nih.gov),
National Institute of Mental Health, Bethesda, Maryland, USA

[76] S Lorin, E Grusell, N Tilly, J Medin, P Kimstrand and B Glimelius Reference dosimetry in a scanned pulsed proton beam using ionisation chambers and a Faraday cup
Phys. Med. Biol. 53 (2008) 3519Ð3529.

[77] E Grusell, Isacsson U, Montelius A and Medin J 1995, Faraday cup dosimetry in a proton therapy beam without collimation
Phys. Med. Biol. 40 1831Ð40.

[78] Stopping Powers & Ranges for Protons & Alpha Particles (I C R U Report No 49).
Intl. Commission on Radiation (June 1993).

[79] Boon S N, van Luijk P, Bohringer T, Coray A, Lomax A, Pedroni E, Schaffner B and Schippers J M 2000 Performance of a SSuorescent screen and CCD camera as a two-dimensional dosimetry system for dynamic treatment techniques
Med. Phys. 27 2198Ð208.

[80] Cambria R et al., Proton beam dosimetry: a comparison between the Faraday cup and an ionization chamber
Phys Med Biol. 1997 Jun;42(6):1185-96.

[81] Ledingham K W, Galster W, Sauerbrey R., Laser-driven proton oncology-a unique new cancer therapy
Br J Radiol. 2007 Nov;80(959):855-8.

[82] Fiorini F., Kirby D., Borghesi M., Doria D., Jeynes J.C.G., Kakolee K.F., Kar S., Kaur S., Kirby K.J., et al., Dosimetry and spectral analysis of radiobiological experiment using laser-driven proton beams
Phys. med. Biol. 56, 6969-6982 (2011).

[83] Schell S., Wilkens J.J., Advanced treatment planning methods for efficient radiation therapy with laser accelerated proton and ion beams
Med. Phys. 37 (10), 5330-5340, (2010).

[84] Scampoli P. , Bisogni M.G, Carpentieri C., di Martino F., Durante M., Gialanella G., Giannelli M., Grossi G., Magaddino V., Manti L., Moriello C., Pugliese M., Righi S., BIORT: an experiment for the assessment of the biological effects of of very high

dose rate and dose per pulse electron irradiations
Il Nuovo Cimento C, 31, 3-9 (2008)

[85] Schmid T.E., Dollinger G., Hauptner A.,Hable V., Greubel C., Auer S., Friedl A.A.,Molls M.,Roper B.,

No evidence for a different RBE between pulsed and continuous 20 MeV protons
Radiat. Res. ,172,567-574 (2009)

[86] Schmid T.E., Dollinger G., Hable V., Greubel C., Zlobinskaya O., Michalski D., Auer S., Friedl, A.A., Schmid E., Molls M., Roper B. The effectiveness of 20 MeV protons at nanosecond pulse lengths in producing chromosome aberrations in human-hamster hybrid cells
Radiat. Res. ,175,719-727(2011)

[87] Zlobinskaya O., Dollinger G., Michalski D., Hable V., Greubel C., Du G., Multhoff G,. Roper B., Molls M., Schmid T.E. Induction and repair of DNA double-strand breaks assessed by gamma-H2AX foci after irradiation with pulsed or continuous proton beams
Radiat. Environ. Biophys. ,51, 23-32 (2012).

[88] Schmid T.E., Dollinger G., Hable V., Greubel C., Zlobinskaya O., Michalski D., Molls M., Roper B.

Relative biological effectiveness of pulsed and continuous 20 MeV protons for micronucleus induction in 3D human reconstructed skin tissue
Radiother Oncol. 95, 66-72 (2010).

[89] Auer S., Hable V., Greubel C., Drexler G.A., Schmid T.E,. Belka C., Dollinger G., Friedl A. Survival of tumor cells after proton irradiation with ultra-high dose rates
Radiat Oncol. , 6, 139 (2011)

[90] Berry R. J., Forster D. W., Storr T. H., Goodman M. J. Survival of mammalian cells exposed to x rays at ultra-high dose-rates
Br. J. Radiol. 42, 102-107 (1969).

[91] Hornsey S. and Alper T. Unexpected dose-rate effect in the killing of mice by radiation
Nature, 210, 212-3 (1966).

[92] Field S.B. and Bewley D. K. Effects of dose-rate on the radiation response of rat skin
Int. J. Radiat. Biol. Relat. Stud. Phys.Chem. Med. ,26, 259-67(1974).

[93] Inada T. Nishio H. Amino S., Abe K., Saito K. High dose-rate dependence of early

skin reaction in mouse
Int. J. Radiat. Biol. 38, 139-45 (1980).

[94] Dewey J. L. and Boag J. W. Modification of the oxygen effect when bacteria are given large pulses of radiation
Nature, 183, 1450-1 (1959).

[95] Kraft D.K., Richter C., ,Zeil K., ,MBaumann M., Beyreuther E.,Bock S., Bussmann M.,Cowan T. E., , Dammene Y.,Enghardt W.,Helbig U.,Karsch L., Kluge T.,Laschinsky L.,Lessmann E.,Metzkes J., Naumburger D., Sauerbrey R.,.Sch§rer M. ,Sobiella M.,Woithe J.,Schramm U., Pawelke J. Dose-dependent biological damage of tumour cells by laser-accelerated proton beams.
New J. Phys. , 12, 1-12 (2010).

[96] Yogo A.,Maeda T., Hori T., Sakaki H., Ogura K.,Nishiuchi M.,Sagisaka A., Kiriyama H., Okada H.,Kanazawa S.,Shimomura T.,Nakai Y., Tanoue M.,Sasao F., Bolton P. R.,Murakami M.,Nomura T., Kawanishi S.,Kondo K., Measurement of relative biological effectiveness of protons in human cancer cells using a laser-driven quasimonoenergetic proton beamline
Appl. Phys. Lett., 98, 053701-3 (2011)

[97] Doria D.,Kakolee K. F., Kar S.,Litt S. K., Fiorini F.,Ahmed H.,Green S., Jeynes J. C. G.,Kavanagh J.,Kirby D.,Kirkby K. J., Lewis C. L.,Merchant M. J.,Nersisyan G.,Prasad R.,Prise K. M.,Schettino G.,Zepf M., Borghesi M. Biological effectiveness on live cells of laser driven protons at dose rates exceeding 10^9 Gy/s
AIP Advances, 2, 011209-6 (2012).

[98] Francesconi M., Remondini D., Neretti N., Sedivy J. M., Cooper L. N., Verondini E., Milanesi L.,Castellani: G. Reconstructing networks of pathways via significance analysis of their intersections
BMC Bioinformatics , 25, 9(2008).

[99] Remondini D., O'Connell B., Intrator N., Sedivy J. M., Neretti N. , Castellani G., Cooper L. N. Targeting c-Myc activated genes via a correlation method: Detection of global changes in large gene expression network dynamics
Proc. Natl. Acad. Sci. U S A ,102, 6902-6 (2005).

[100] MUSUMECI F., PRIVITERA G., SCORDINO A., TUDISCO S., LO PRESTI C., APPLEGATE L. A., NIGGLI H. J. Discrimination between normal and cancer cells by using spectral analysis of delayed luminescence
Appl. Phys. Lett. 86 , 153902-04 (2005)

[101] BARAN I.,GANEA C., SCORDINO A., MUSUMECI F., BARRESI V., TUDISCO S., PRIVITERA S., GRASSO R., CONDORELLI D. F., BARAN V., KATONA E., MOCANU M-M., GULINO M., UNGUREANU R., SURCEL M.,URSACIUC C. Effects of menadione, hydrogen peroxide and quercetin on apoptosis and delayed luminescence of human leukemia Jurkat T-cells
Cell Biochem. Biophys. 58, 169-179 (2010)

[102] BARAN I.,GANEA C., PRIVITERA S., SCORDINO A., BARRESI V., MUSUMECI F.,MOCANU M.-M. CONDORELLI D. F., URSU I., GRASSO R., GULINO M., GARAIMAN A., MUSSO N., CIRRONE G.A.P.,CUTTONE G. Detailed analysis of apoptosis and delayed luminescence of human leukemia Jurkat Tcells after proton-irradiation and treatments with oxidant agents and flavonoids
Oxidative Med. Cell. Longevity (2012)

[103] Dzalainis et al., *Proc. of SPIE Vol. 7451 45119-2*

[104] Dzalainis et al., *Laser and Particles Beams, 2010 doi: 10.1017/S026303*

[105] G. E. Cook, *Pulse Compression-Key to More Efficient Radar Transmission*, IEEE Proc. IRE 48, 310 (1960)

[106] D. Strickland and G. Mourou, Compression of amplified chirped optical pulses
Opt. Commun. 56, 219 (1985)

[107] S. Eliezer, The Interaction of High-Power Laser with Plasmas
IOP Publishing Ltd, 2002.

[108] P. Gibbon, Short Pulse Laser Interaction with Matter
Imperial College Press, 2005.

[109] M. Passoni, L. Bertagna, A. Zani, Target normal sheath acceleration: theory, comparison with experiments and future perspective
New J. Phys. 12 045012 (2010).

[110] A. Macchi and C. Benedetti, Ion acceleration by radiation pressure in thin and thick targets
Nucl. Inst. Meth. Phys. Res. A (2010) DOI: M10.1016/j.nima.2010.01.057

[111] I. Petrovic, A. Ristic-Fira, D. Todorovic, L. Valastro, P. Cirrone, G. Cuttone, Radiobiological analysis of human melanoma cells on the 62 MeV CATANA proton beam
International Journal of Radiation Biology, 82(4): 251-265, (2006).

[112] I. Petrovic, A. Ristic-Fira, D. Todorovic, L. Koricanac, L. Valastro, G.A.P. Cirrone, G. Cuttone. Response of a radio-resistant human melanoma cell line along the proton

spread-out Bragg peak
International Journal of Radiation Biology, 86(9): 742-751, (2010).

[113] A. Ristic-Fira, D. Todorovic, J. Zakula, O. Keta, P. Cirrone, G. Cuttone, I. Petrovic. Cellular Response to Conventional Radiation and Hadrons
Physiological research, 60: 129-135, (2011).

[114] A. Ristic-Fira, L. Koricanac, J. Zakula, O. Keta, G. Iannolo, G. Cuttone, I. Petrovic. Proton inactivation of melanoma cells enhanced by fotemustine
Radiation Protection Dosimetry, 143: 503-507, (2011).

[115] L. Koricanac, J. Zakula, G. A. P. Cirrone, G. Privitera, G. Cuttone, I. Petrovic, A. Ristic-Fira. Variation of apoptotic pathway regulators by fotemustine and protons in a human melanoma cell line
Advanced Science Letters, 5: 552-559, (2012).